Journal Pre-proofs

Effect of particle size on the dispersion behavior of magnesium stearate blended with microcrystalline cellulose

Daniel Puckhaber, Jan Henrik Finke, Sarah David, Bindhumadhavan Gururajan, Supriya Rane, Arno Kwade

PII: S0378-5173(24)00026-7
DOI: https://doi.org/10.1016/j.ijpharm.2024.123792
Reference: IJP 123792

To appear in: *International Journal of Pharmaceutics*

Received Date: 4 October 2023
Revised Date: 4 January 2024
Accepted Date: 4 January 2024

Please cite this article as: D. Puckhaber, J. Henrik Finke, S. David, B. Gururajan, S. Rane, A. Kwade, Effect of particle size on the dispersion behavior of magnesium stearate blended with microcrystalline cellulose, *International Journal of Pharmaceutics* (2024), doi: https://doi.org/10.1016/j.ijpharm.2024.123792

Effect of particle size on the dispersion behavior of magnesium stearate blended with microcrystalline cellulose

Daniel Puckhaber[1,2], Jan Henrik Finke[1,2*], Sarah David[3], Bindhumadhavan Gururajan[3], Supriya Rane[3] and Arno Kwade[1,2]

[1] Institute for Particle Technology, Technische Universität Braunschweig, Volkmaroder Straße 5, 38104 Braunschweig, Germany

[2] Center of Pharmaceutical Engineering (PVZ), Technische Universität Braunschweig, Franz-Liszt-Straße 35A, 38106 Braunschweig, Germany

[3] Novartis Pharma AG, Basel 4002, Switzerland

*Correspondence: j.finke@tu-braunschweig.de

Abstract:

The majority of tablets manufactured contain lubricants to reduce friction during ejection. However, especially for plastically deforming materials, e.g., microcrystalline cellulose (MCC), the internal addition of lubricants is known to reduce tablet tensile strength. This reduction is caused by the surface coverage by lubricant particles, the extent of which depends on both process and formulation parameters. Previously published models to predict the lubrication effect on mechanical strength do not account for changes in the excipient particle size. In this study, the impact of both lubricant concentration and mixing time on the tensile strength of tablets consisting of three different grades of MCC and four grades of magnesium stearate (MgSt) was evaluated. By taking into account the particle size of the applied excipients, a unifying relationship between the theoretically estimated surface coverage and compactibility reduction was identified. Evaluating the dispersion kinetics of MgSt as a function of time reveals a substantial impact of the initial surface coverage on the dispersion rate, while the minimal tensile strength was found to be comparable for the majority of formulations. In summary, the presented work extends the knowledge of lubricant dispersion and facilitates the reduction of necessary experiments during the development of new tablet formulations.

Keywords: tableting, magnesium stearate, lubrication, dispersion behavior, particle size

1. Introduction

The majority of industrial tablet formulations contain particulate lubricants, which facilitate tablet ejection by reducing the interfacial friction between the lateral tablet surface and inner die wall. However, the internal addition of lubricants is known to bear the risk of reducing the mechanical tablet strength [1–5]. The reduction in mechanical strength is caused by the coverage of the surfaces of matrix-forming diluent particles with lubricant particles [5,6]. The extent of mechanical strength reduction strongly depends on the deformation behavior of the lubricated material [1]. Plastically deforming materials are especially sensitive to lubrication, as they typically generate only a limited amount of fresh, unlubricated surfaces during compaction [7,8]. Thus, the coverage of diluent surfaces by lubricant particles may critically affect the interparticulate interactions if excessive amounts of lubricants are added. In contrast, brittle fracturing excipients generate substantial amounts of new particle surfaces during compaction, which explains their insensitivity towards lubrication with regard to their mechanical tablet strength [9,10]. Generally, produced tablets must exhibit sufficient mechanical strength to enable successful subsequent processing (such as transport, coating, and packaging) into commercial medicines [11]. Consequently, for plastically deforming materials, in-depth knowledge of the correlation between lubricant surface coverage and mechanical tablet strength is necessary to reduce the number of time- and cost-intensive experiments during the development of new tablet formulations.

It is generally agreed that the detrimental effect of lubricant addition on mechanical strength is based on the surface coverage by lubricant particles [5,6,12–14]. There has been a substantial effort to

characterize the underlying mechanisms and extent of surface coverage by lubricant particles experimentally using different measurement techniques.

The majority of studies focused on the investigation of the distribution of magnesium stearate (MgSt), which is the predominantly applied pharmaceutical lubricant. Initial studies applied scanning electron microscopy (SEM) to investigate the distribution of MgSt on surfaces, which showed a sufficient contrast to identify MgSt particles [5,6]. By combining SEM and energy dispersive X-ray analysis, the surface coverage of NaCl [12] and API crystals [15] was quantitatively evaluated. Additionally, secondary ion mass spectometry [16] and raman spectroscopy [17] were found to be suitable to quantify the distribution of MgSt. All these methods have in common that the determination of surface coverage by lubricant particles is experimentally very laborious and has therefore only been carried out for selected substance combinations in order to elucidate fundamental mechanisms.

Generally, the extent to which the lubricant addition affects tablet properties depends on the type of applied lubricant [18–20], the lubricant amount [1,20], the lubricant particle size [21], the applied mixing device [4,22], the mixing time [2,13] and, if applied, the paddle feeder passage [23–25]. The high number of influencing factors and their complex interplay hinders, so far, the development of generally applicable models that are capable of precisely predicting the impact of lubrication on the final tablet tensile strength. Thus, previous research has been focused on developing suitable methods to characterize individual sub-processes.

The most prominent model to capture the effect of lubrication on tablet strength was introduced by Kushner et al. [4,26,27]. They developed a mathematical model that allows for scaling-up the mixing process for lubricated formulations in free-fall mixers by taking into account the effects of several process parameters (blender volume, headspace, and number of blender revolutions). However, as pointed out by the authors themselves, their model is not able to capture the effect of changes in the formulation. Thus, if the formulation is altered, time-consuming experiments to reparametrize the model are necessary, which are economically unfavorable.

The effect of lubricant concentration on the reduction of compactibility was recently quantitatively modeled by our research group by introducing an empirical model for binary formulations [28]. Subsequently, the model was combined with the model of Reynolds et al. [29] and, by that, extended to more complex formulations [30]. The effect of lubricant concentration on structural and mechanical tablet properties was modeled by theoretically estimating the surface coverage based on the initial particle size distributions of applied excipients. However, the experiments were limited to very short mixing times in a given blender setup, and by that, only a limited process setup was investigated. Generally, it would be desirable to extend the available formulation knowledge in order to predict the extent to which the mechanical strength is altered if one excipient is replaced with another grade exhibiting a different particle size.

Therefore, in this study, a comprehensive evaluation of the mechanical strength of binary tablets consisting of MCC and MgSt of different particle sizes for various lubricant concentrations and mixing times was performed. By calculating the theoretical surface coverage of MCC particles by lubricant particles, a unifying relationship between theoretical surface coverage and compactibility reduction due to lubrication independent of the applied excipient particle size was derived for short mixing times. Afterwards, for a given lubricant concentration, blending experiments, in which the mixing time was greatly varied between 2 – 600 min, were executed, and the derived compactibility reduction was modeled by adapting the dispersion model proposed by Schilde et al. [31].

2. Methods and Materials

2.1 Particle size analysis

Particle size distributions were measured by means of laser diffraction (MasterSizer 3000, Malvern Panalytical, USA). Powders were dispersed by using the dry dispersion unit AERO S and applying a dispersion pressure of 0.5 bar. Samples were measured in triplicate, and an average particle size

distribution was calculated. Additionally, the specific surface area $S_{m,LD}$ was calculated based on the particle size distribution and considering the solids density ρ_s.

2.2 Solids density

Solids densities ρ_s were measured by means of helium pycnometry (Ultrapyc 1200e, Micromeritics, USA). For each material, three samples were investigated in a ten-fold measurement and an average solids density was calculated.

2.3 Scanning election microscopy

Particle morphology was investigated by means of scanning electron microscopy (SEM; Helios G4 CX, Thermo Fisher Scientific, USA). Samples were sputtered with gold (LEICA EM ACE600, Leica microsystems GmbH, Germany).

2.4 Gas adsorption analysis

Specific surface areas of lubricants were analyzed by gas adsorption measurements (ASAP 2460, micromeritics, USA) applying the 5-point BET method. Samples were conditioned under vacuum at 25 °C overnight. Nitrogen was used as an adsorptive. Powders were analyzed in triplicate and an average specific surface area $S_{m,BET}$ was calculated.

2.5 Blending

Blends of 50 g were produced by means of a Turbula mixer (T2F, Willy A. Bachofen GmbH, Germany) using 1 L glass bottles. For all blends, a rotation frequency of 49 min^{-1} was applied. The effect of lubricant concentration on the mechanical tablet strength was evaluated by systematically varying the lubricant concentration between 0.25 and 2 wt.% and applying a mixing time of 2 min. In order to examine the effect of mixing time on mechanical strength, binary blends of MCC and MgSt were produced with a fixed lubricant concentration of 0.5 wt.% for varying mixing times (2 – 600 min). Additionally, binary blends of MCC and MgSt with very small to medium amounts of MgSt (0.02 – 1 wt.%) were produced by applying a mixing time of 120 min.

2.6 Compaction

Tablets were produced by a compaction simulator (Stylone evolution, Medelpharm, France), which was equipped with 11.28 mm round, flat-faced tooling. In the case of formulations containing MCC_{fine} or MCC_{medium}, dies were filled by hand after manually weighing the desired powder mass. For MCC_{coarse}, a gravity feeder was applied to fill the dies. Independently of the filling method, a tablet weight of approximately 450 mg was used. The compression profile of a StylCam (Medelpharm, France) with a rotation frequency of 5 min^{-1} was simulated. The compression stress was systematically varied between 50 and 300 MPa. For each set of process parameters, five tablets were produced and stored under lab conditions (20 ± 1 °C, 40 ± 10% r.H.).

2.7 Tablet analysis

After measuring the tablet weight m_t, the tablet height h_t and tablet diameter d_t were determined by a tablet tester (MultiTest 50 FT, Dr. Schleuniger, Switzerland). By relating the resulting tablet density ρ_{tablet} to the solids density ρ_s, the tablet porosity ε was calculated:

$$\varepsilon = 1 - \frac{\rho_{tablet}}{\rho_s} = 1 - \frac{4 \cdot m_t}{\pi \cdot d_t^2 \cdot h_t \cdot \rho_s} \quad (1)$$

Afterwards, the tablet breaking force F_B was measured by a diametral compression test (MultiTest 50 FT, Dr. Schleuniger, Switzerland) with a loading rate of 0.35 mm s^{-1}. The resulting tablet tensile strength σ_t was calculated according to the equation of Fell and Newton [32]:

$$\sigma_t = \frac{2 \cdot F_B}{\pi \cdot d_t \cdot h_t} \quad (2)$$

2.8 **Materials**

Three different grades of microcrystalline cellulose (Vivapur 101 (MCC_{fine}), Vivapur 102 (MCC_{medium}) and Vivapur 200 (MCC_{coarse}), all JRS Pharma, Germany) were considered in this study. For lubrication, four different grades of magnesium stearate (Carl Roth, Germany ($MgSt_1$); Faci, Italy ($MgSt_3$); Ligamed MF-2-V, Peter Greven GmbH, Germany ($MgSt_2$); Ligamed MF-3-V, Peter Greven GmbH, Germany ($MgSt_4$)) were used. Prior to application, lubricants were deagglomerated by using a 355 µm sieve.

The morphology and particle size of the investigated lubricants were investigated by means of SEM images. The nomination of MgSt grades follows their median particle size (cf. Figure 1 and Figure 2b). $MgSt_2$, $MgSt_3$, and $MgSt_4$ exhibit a comparable particle morphology in which the platelet-shaped primary particles are agglomerated into coarser secondary particles. It is generally believed that during blending processes, acting shear stress results in the dispersion of these primary lubricant particles for prolonged mixing times [5,33]. In contrast, $MgSt_1$ consists of considerably larger primary particles, which showed a limited surface roughness to which smaller particles are attached. Generally, all investigated MgSt grades exhibit a monomodal particle size distribution whereby the median particle size ranges between 17.2 µm ($MgSt_1$) and 6.9 µm ($MgSt_4$) (Table 1 and Figure 2).

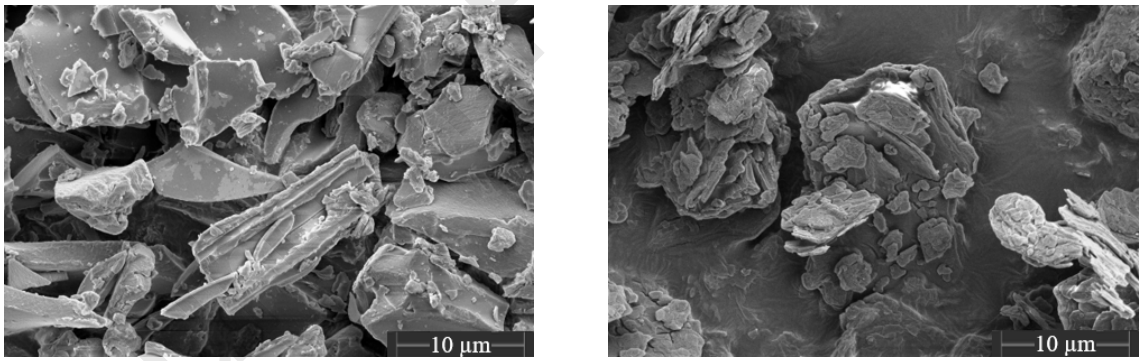

(a) (b)

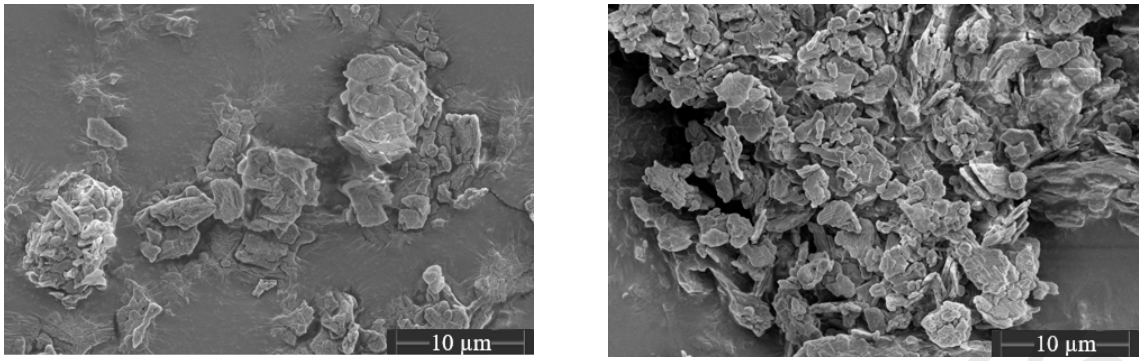

(c) (d)

149 Figure 1: SEM images of $MgSt_1$ (a), $MgSt_2$ (b), $MgSt_3$ (c) and $MgSt_4$ (d)

150 The applied MCC grades possess considerably larger particles, as shown in Figure 2a. The cumulative
151 particle size distributions revealed expected differences between the applied MCC grades, as the median
152 particle sizes significantly differed between 70 µm (MCC_{fine}) and 261 µm (MCC_{coarse}) (Table 1).

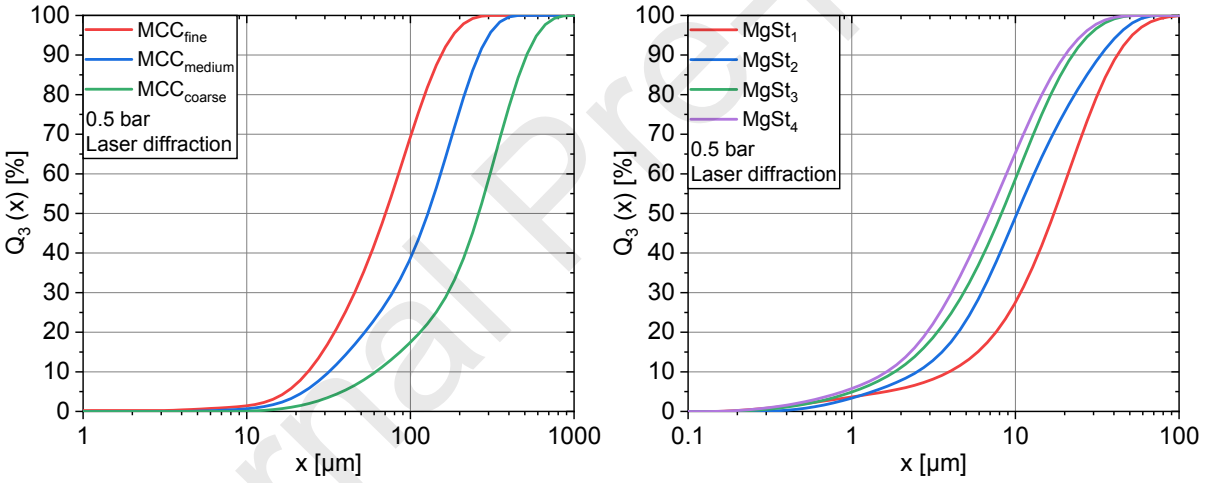

(a) (b)

153 Figure 2: Cumulative particle size volume distributions of the investigated grades of MCC (a) and MgSt
154 (b) determined by laser diffraction for a dispersion pressure of 0.5 bar.

155 Additionally, the specific surface areas of the lubricants determined by gas adsorption substantially
156 differ between 0.95 $m^2\ g^{-1}$ ($MgSt_1$) and 34.45 $m^2\ g^{-1}$ ($MgSt_4$) and do not follow the order of median
157 particle size. This discrepancy can be attributed to the different primary particle size of the lubricant
158 particles examined which determine the $S_{m,BET}$ values. Contrarily, the x_{50} values correspond to the
159 secondary particle size of the visible lubricant agglomerates. Thus, the investigated lubricants show
160 significant differences in their particulate structure, the influence of which on the dispersion behavior is
161 investigated in this study.

162 Table 1: Bulk properties of investigated diluents and lubricants. Specific surface area values represent
163 average values ± standard deviation.

Diluent	x_{50} [µm]	Lubricant	x_{50} [µm]	$S_{m,BET}$ [m^2 g^{-1}]
MCC_{fine}	70 ± 0.1	$MgSt_1$	17.2 ± 0.07	0.95 ± 0.05
MCC_{medium}	128 ± 1.4	$MgSt_2$	10.2 ± 0.03	14.14 ± 0.3
MCC_{coarse}	261 ± 9.9	$MgSt_3$	8.2 ± 0.07	3.18 ± 0.09
		$MgSt_4$	6.9 ± 0.33	34.45 ± 3.1

3. Results and Discussion

3.1 Impact of lubricant concentration on mechanical strength of tablets

In a first step, the impact of lubrication on the mechanical strength of MCC tablets was investigated by applying short mixing times of 2 min and systematically varying the MgSt concentration between 0.25 and 2 wt.%. Here, the relationship between tablet porosity and tensile strength, the compactibility, was evaluated. The compactibility is only slightly impacted by changes in compaction kinetics [34] and thus, can be seen as a fundamental relationship that describes the bondability of the formulation. Rumpf's model suggests that the bondability of a compact depends on the quantity and strength of bonds formed on the aggregate [35] and can be calculated based on porosity, coordination number, particle surface area, and bonding force.

The internal lubricant addition results in the surface coverage of diluent particles by lubricant particles [5,6]. In the case of lubricated MCC, it can be hypothesized that the negative impact on mechanical strength can be explained by two different mechanisms [36]: First, the presence of lubricants on the surface acts as a physical barrier, preventing, amongst other adhesive forces, strong hydrogen bonding between MCC particles [37] and replacing them with weaker bonding between lubricant and MCC particles. Second, the decreased bonding force of lubricated MCC particles enhances the extent of relaxation during decompression [38] and by doing so, increases the interparticulate distance, reducing effective particle interaction areas.

In this study, MCC was applied as a model material, as its tensile strength is highly sensitive to the addition of lubricants [39], especially due to the limited generation of new, unlubricated surfaces during compaction [7,8]. Consequently, this high sensitivity enables the correlation of the dispersion behavior of MgSt with the process and formulation parameters used in this study. As expected, increasing the concentration of internally applied lubricants results in a severe decrease in the compactibility of binary formulations of MCC and MgSt (Figure 3).

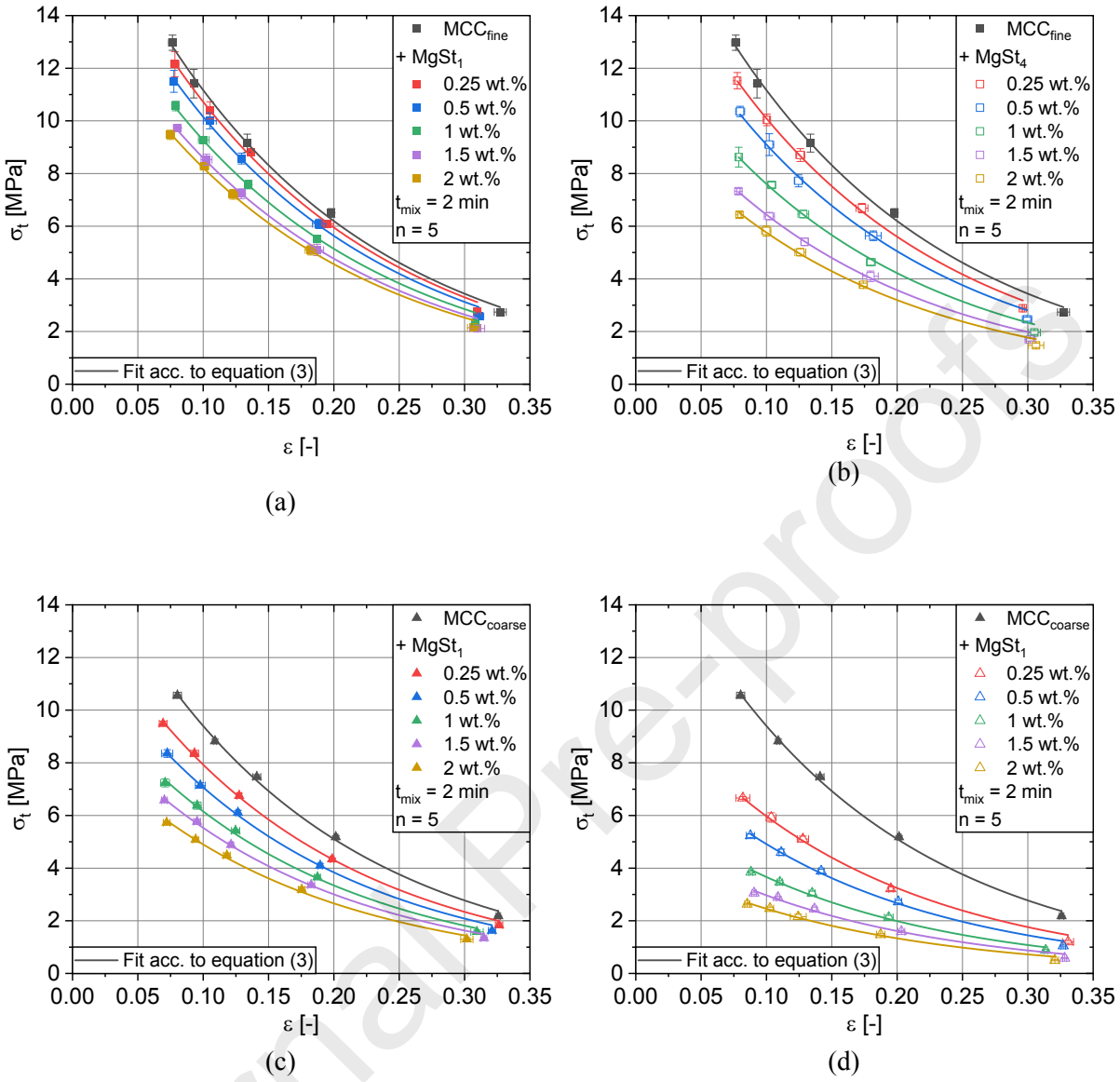

188 Figure 3: Compactibility plots of binary formulations of MCC and MgSt for different lubricant
189 concentrations and a mixing time of 2 min. Lines represent fits acc. to equation (3) with a fixed k_b value
190 determined from the unlubricated MCC grades, named $k_{b,dil}$ (a) MCC$_{fine}$ + MgSt$_1$ (b) MCC$_{fine}$ + MgSt$_4$
191 (c) MCC$_{coarse}$ + MgSt$_1$ (d) MCC$_{coarse}$ + MgSt$_4$

192 The compactibility of tablets was quantified by applying the equation of Ryshkewitch-Duckworth
193 [40,41]:

$$\sigma_t = \sigma_0 \cdot e^{-k_b \cdot \varepsilon} \quad (3)$$

194 Where σ_0 is the theoretical maximal tensile strength for a non-porous tablet and k_b is the bonding
195 capacity.

196 In a previous study of our research group, it was shown that the k_b values of lubricated MCC grades are
197 virtually constant for different MgSt concentrations [28]. Thus, in order to limit the effect of lubrication
198 to the reduction of σ_0, the compactibility profiles of lubricated MCC formulations are fitted by the

Ryshkewitch-Duckworth equation while using the k_b values of the unlubricated diluents $k_{b,dil}$, respectively. The empirical fit parameters of the unlubricated MCC grades were determined beforehand based on their compactibility profiles (Figure S1) and are enlisted in Table 2.

Table 2: Determined parameters of the Ryshkewitch-Duckworth equation for unlubricated MCC grades

Diluent	Bonding capacity k_b [-]	Theoretical max. tensile strength σ_0 [MPa]
MCC_{fine}	5.89 ± 0.24	20.12 ± 0.57
MCC_{medium}	5.9 ± 0.23	18.55 ± 0.54
MCC_{coarse}	6.1 ± 0.21	17.3 ± 0.45

As expected and already shown in a previous publication [28], the subsequently derived theoretical maximal tensile strength values decrease for rising lubricant concentrations (Figure 4). Obviously, if finer MgSt grades (e.g., $MgSt_4$) are applied, smaller σ_0 values result for a given lubricant concentration. This detrimental effect of smaller lubricant particles on the mechanical tablet strength is well known [21,42] and can be explained by the higher number of lubricant particles for a given lubricant concentration, resulting in a higher coverage of diluent particles. Consequently, a greater fraction of comparably stronger MCC-MCC bonds is replaced by weak MCC-MgSt or MgSt-MgSt bonds and by that, the tablet strength decreases. Additionally, for a given lubricant grade and concentration, the application of coarser MCC particles results in a considerably higher reduction of compactibility (cf. Figure 4a and Figure 4c). This effect is caused by the smaller available diluent surface, which, if the same number of lubricant particles are applied, will be covered to a greater extent by lubricant particles. It is obvious that the extent of compactibility reduction depends on both applied diluent and lubricant particle size for binary formulations of MCC and MgSt, due to the different resulting surface coverages. In previously conducted studies [21,42], the same qualitative explanatory approach was used, but no quantitative correlation taking into account the particle sizes of both excipients was derived.

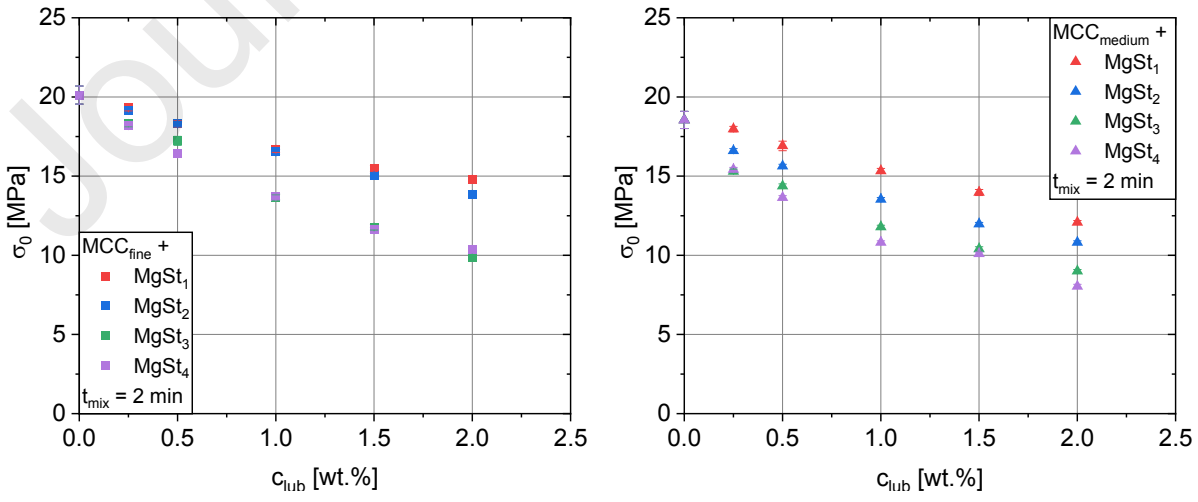

(a) (b)

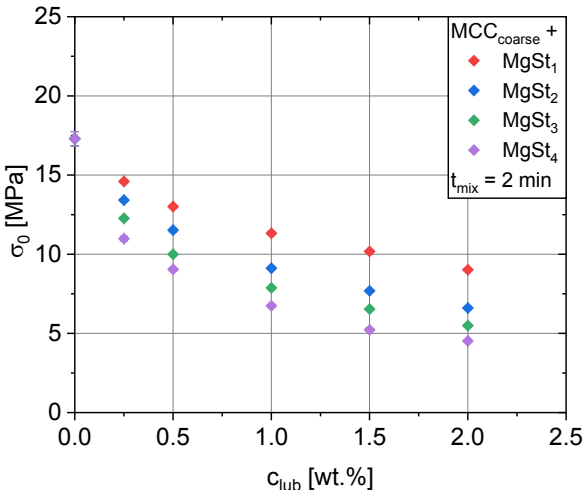

(c)

Figure 4: Correlation of lubricant concentration and theoretical max. tensile strength σ_0 for binary mixtures of MCC_{fine} (a), MCC_{medium} (b), MCC_{coarse} (c) and four different grades of MgSt for a mixing time of 2 min.

Measuring the extent of surface coverage by lubricant particles is experimentally challenging and time-consuming. As discussed above, quantitative values of surface coverage by MgSt are typically based on SEM measurements. However, identifying MgSt on MCC particles is extremely challenging as the debris of MCC and MgSt exhibit comparable morphologies [5] and MCC particles do not exhibit the required smooth particles surfaces [15].

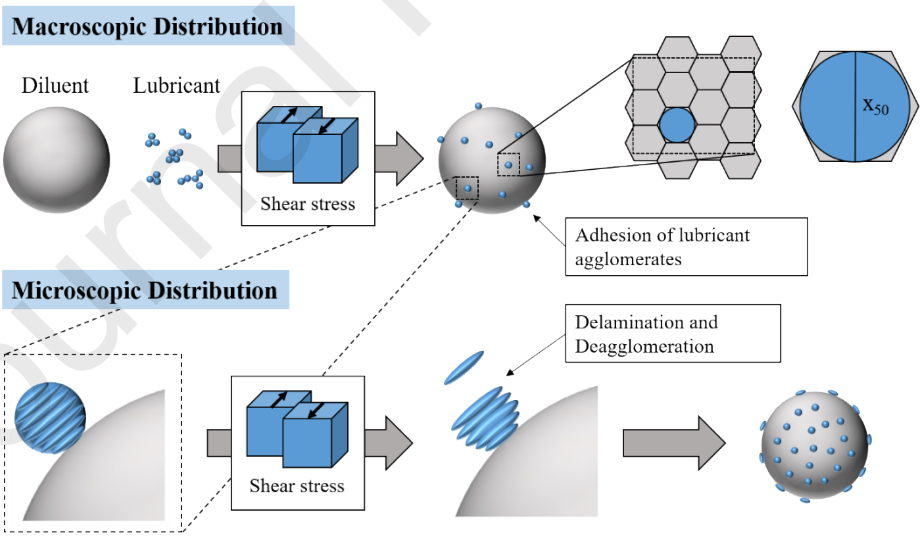

Figure 5: Schematic representation of the proposed dispersion mechanisms during mixing of MgSt and diluent particles. Initially, lubricant agglomerates adhere to the diluent surface and occupy a hexagonal shaped area according to their x_{50}. If further shear stress is applied, MgSt particles deagglomerate or delaminate into platelets, which consecutively cover additional diluent surfaces.

In the course of this study, the dispersion mechanisms proposed by Shah and Mlodozeniec are considered [5]. The dispersion of MgSt due to shear stress can thereby be distinguished in two consecutive steps: First MgSt stearate agglomerates adhere to the diluent surfaces resulting in a macroscopic distribution of the lubricant. If further shear stress is applied, the lubricant agglomerates

deagglomerate or delaminate, due to their lamellar structure, into smaller particles and which consecutively cover additional diluent surfaces (Figure 5).

The resulting macroscopic lubricant distribution was theoretically estimated by calculation of the geometric surface coverage according to the approach of Meyer [43]. It is assumed that each lubricant particle occupies a hexagonal area on the diluent surface according to its median particle size x_{50} (Figure 5). For this methodology, several assumptions are drawn:

1. For short mixing times, the lubricant agglomerates are distributed on the diluent surfaces due to acting shear stresses and occupies the diluent surface. No further deagglomeration or delamination has taken place.
2. The different lubricant particle sizes after the macroscopic distribution can be represented by a characteristic particle size (x_{50}), which can reliably be measured by laser diffraction.
3. The available diluent surface can be estimated by the specific surface area calculated from particle size distributions measured by laser diffraction.
4. The deposition of lubricant agglomerates on free diluent surfaces is favored in terms of the formation of lubricant multilayer on the diluent surface

Naturally, those assumptions do not represent the distributed nature of particle properties of both diluents and lubricants as well as the irregular shape of those entities. However, in a previous publication, this approach was successfully applied to link the effect of lubrication to the prediction of multi-component mixtures [30] and to identify a common relationship between compactibility reduction and lubricant particles size of chemically different lubricants [19].

The total available diluent surface S_{dil} can be calculated by multiplying the specific surface area $S_{m,LD}$ with the total diluent mass m_{dil}:

$$S_{dil} = S_{m,LD} \cdot m_{dil} \quad (4)$$

The occupied area by lubricant particles S_{lub} can be derived by [43]:

$$S_{lub} = n_{lub} \cdot S_{lub,particle} = \left(\frac{m_{lub}}{\frac{\pi}{6} \cdot x_{50,lub}^3 \cdot \rho_{s,lub}} \right) \cdot \frac{\sqrt{3}}{2} \cdot x_{50,lub}^2 \quad (5)$$

Where $x_{50,lub}$ is the median particle size of the investigated lubricant and m_{lub} is the total lubricant mass. Afterwards, the particle size-based theoretical surface coverage SC_{theo} can be calculated:

$$SC_{theo} = \frac{S_{lub}}{S_{dil}} \quad (6)$$

By relating SC_{theo} to σ_0 values of lubricated blends, a unifying relationship for binary blends of a given MCC grade and different MgSt grades was identified (Figure 6a-c). For all applied MCC grades, an exponential decrease of σ_0 for rising SC_{theo} values was observed.

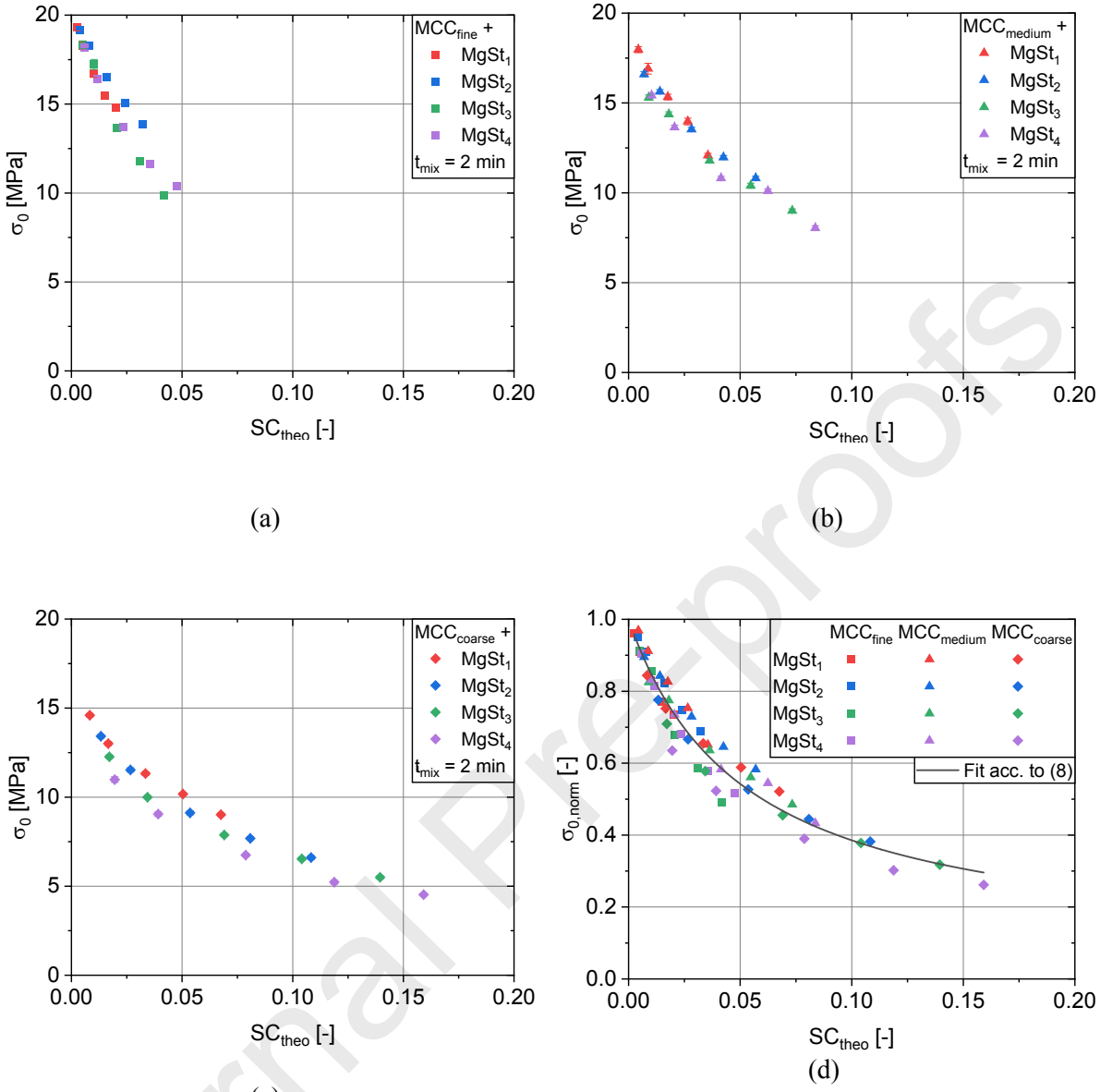

Figure 6: Correlation between σ_0 and SC_{theo} for binary blends of MCC_{fine} (a), MCC_{medium} (b), MCC_{coarse} (c) and four different grades of MgSt. Correlation between $\sigma_{0,norm}$ and SC_{theo} for all investigated blends of three different MCC and four different MgSt grades (d).

In case of unlubricated MCC tablets, despite being generally comparable, a slight trend of higher σ_0 values for finer MCC grades was determined (Table 2). This difference in initial compactibility impedes the direct comparison of σ_0 values of lubricated MCC grades. In order to allow a meaningful comparison of different grades, the derived $\sigma_{0,lub}$ values of lubricated formulations were normalized by the $\sigma_{0,dil}$ values of the unlubricated MCC grade, respectively:

$$\sigma_{0,norm} = \frac{\sigma_{0,lub}}{\sigma_{0,dil}} \quad (7)$$

Plotting $\sigma_{0,norm}$ against SC_{theo} reveals a unifying compactibility reduction for higher SC_{theo} values. This finding indicates that the initial MgSt dispersion is governed by the macroscopic distribution of lubricant agglomerates, as previously assumed [5], and depends on the initial particle sizes of applied excipients. The reduction of $\sigma_{0,norm}$ was modeled by fitting the data with an appropriate dispersion kinetic. Here, the dispersion kinetic published by Schilde et al. was adapted [31], which depicts a modified Michaelis-Menten kinetic:

$$\sigma_0 = \sigma_{0,dil} + (\sigma_{0,end} - \sigma_{0,dil}) \cdot \frac{SC_{theo}}{SC_{theo} + K_{Macro}} \quad (8)$$

Where $\sigma_{0,end}$ describes the minimal σ_0 value and K_{Macro} represents an empirical kinetic constant. By considering equation (7), equation (9) can be yielded:

$$\sigma_{0,norm} = 1 + (\sigma_{0,end,norm} - 1) \cdot \frac{SC_{theo}}{SC_{theo} + K_{Macro}} \quad (9)$$

Generally, it can be hypothesized that the minimal value of $\sigma_{0,norm}$ should be close to zero due to the weak interactions between MgSt particles, however, results shown in later chapters indicate that the threshold value will most likely be different to zero. Additionally, it is questionable if the threshold can be reasonably assessed, as a further increase of SC_{theo} resulted in obvious tablet defects. As the investigated lubricant concentrations are well within the industrially applied range, higher lubricant concentrations were not examined.

Generally, alternative dispersion models [4,23] were also evaluated, but resulted in poorer correlation (data not shown). As shown in Figure 6d, the adapted dispersion kinetic accurately describes the plotted data ($R^2 \sim 0.95$) and thereby, once parametrized by a limited number of experiments, can be used to predict the compactibility loss due to lubrication of MCC for different excipient particle sizes. However, as 12 individual combinations of materials are taken into account, a maximum deviation of approx. 15% of single values from the model occurs. Consequently, the proposed approach represents an interesting tool for formulation development, as it requires only comparatively easily measurable particle properties and allows the adaptation to partially unavoidable changes in the starting material quality.

3.2 Impact of mixing time on mechanical strength of tablets

The interplay of MgSt and MCC particle sizes on the dispersion behavior of MgSt for prolonged mixing times was evaluated by creating binary formulations with a fixed MgSt concentration of 0.5 wt.% and systematically varying the mixing time between 2 and 600 min. For longer mixing times, it is proposed that MgSt deagglomerates and delaminates resulting in an increased coverage of MCC surfaces (Figure 5). Accordingly, with increased mixing time, the compactibility is reduced (Figure S2) and can be quantified by applying the Ryshkewitch-Duckworth equation (3). Analogous to the impact of lubricant concentration, the $k_{b,dil}$ value of the unlubricated MCC grades was used to limit the effect of lubricant addition to σ_0. Subsequently, the σ_0 vs. t_{mix} plots were evaluated by applying the adapted dispersion kinetic of Schilde et al. [31]:

$$\sigma_0 = \sigma_{0,dil} - (\sigma_{0,dil} - \sigma_{0,end}) \cdot \frac{t_{mix}}{t_{mix} + K_{Micro}} \quad (10)$$

Where K_{Micro} is a kinetic constant describing the half life time until 50% of the absolute difference between $\sigma_{0,dil}$ and $\sigma_{0,end}$ is reached. The compactibility for a mixing time of 0 min was estimated by applying the σ_0 value of the unlubricated diluent $\sigma_{0,dil}$. The $\sigma_{0,dil}$ values have been quantified beforehand (Table 2), leaving only $\sigma_{0,end}$ and K_{Micro} to be determined.

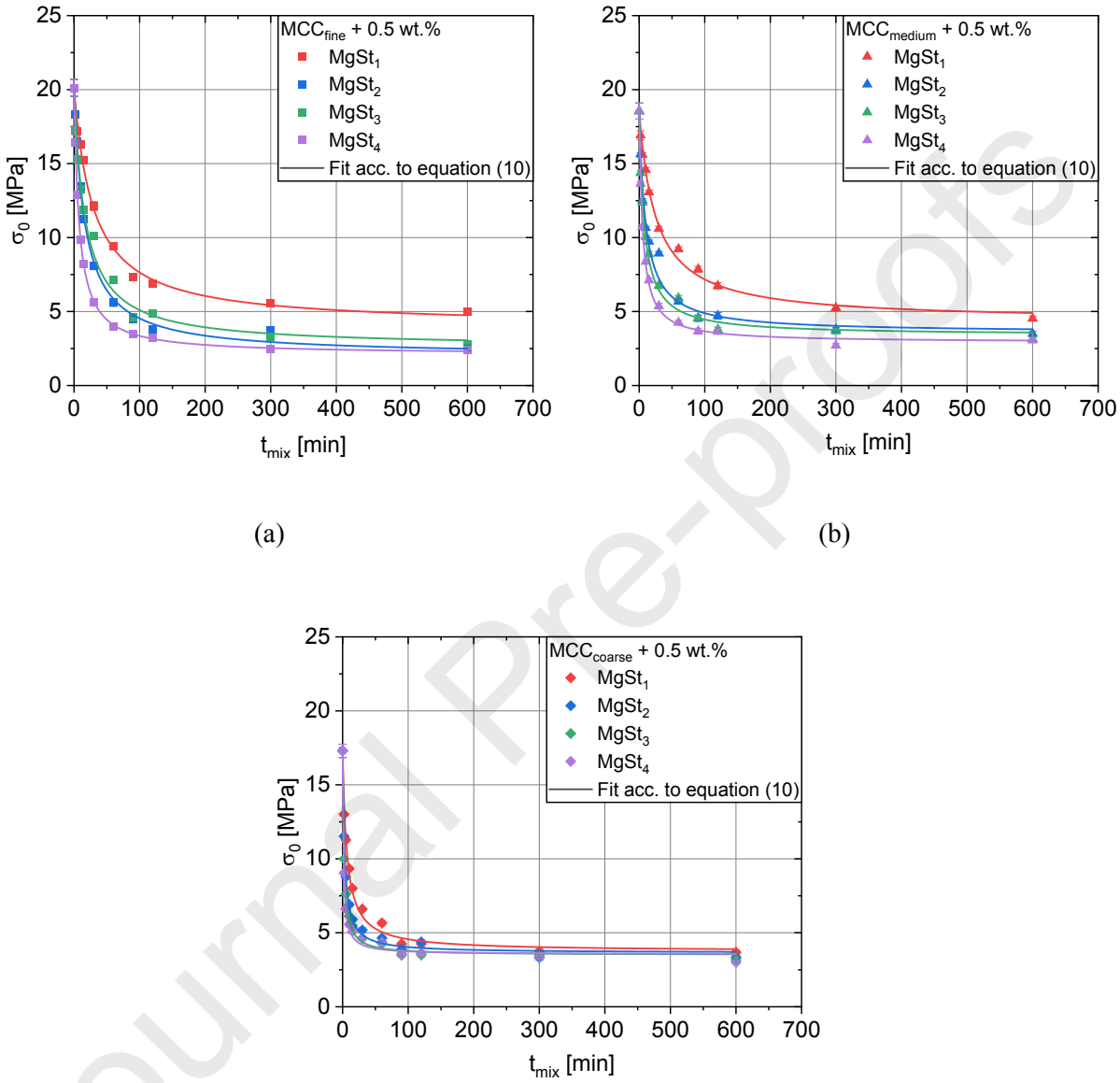

Figure 7: Effect of mixing time t_{mix} on σ_0 values of binary blends of MCC_{fine} (a), MCC_{medium} (b), MCC_{coarse} (c) and different grades of MgSt for a lubricant concentration of 0.5 wt.%. The σ_0 value for a mixing time of 0 min was estimated by $\sigma_{0,dil}$.

As shown in Figure 7, the determined σ_0 values decrease with rising mixing time whereby two phases can be identified: A drastic reduction rate for short mixing times followed by a considerably smaller reduction rate for long mixing times. This reduction rate represents the lubricant dispersion rate. Generally, the majority of investigated formulations approach a common threshold ($\sigma_{0,end}$) between 2.5 – 4 MPa for all investigated formulations. Contrary to this finding, if $MgSt_1$ in combination with MCC_{fine} or MCC_{medium} is applied, the minimum σ_0 value is slightly higher. Those visible differences are not completely resembled by the $\sigma_{0,end}$ values due to the extrapolating nature of the applied fit function (Figure 8a).

The minimal compactibility for long mixing times can be interpreted as an equilibrium state of lubricant dispersion. Assuming that the mixing time of 600 min excludes a limitation due to an insufficient number of stress events, three different scenarios can be envisioned (amongst others) to explain this equilibrium state:

1) The shear stress is insufficient to induce further MgSt delamination due to an increase of shear strength with decreasing particle size of MgSt during mixing. The equilibrium state reflects the maximum surface coverage depending on the lubricant shear strength, lubricant mass and available diluent surface.
2) The shear stress exceeds the shear strength of MgSt at any given time during mixing, resulting in a complete dispersion of the applied MgSt mass. The resulting number and size of MgSt particles is insufficient to cover the available MCC surface. The equilibrium state is defined by the lubricant mass and available MCC surface.
3) The shear stress is sufficiently high to disperse MgSt into particles, which size and number is sufficient to cover the available MCC surface. The equilibrium state is defined by the remaining bonding potential of lubricated MCC surfaces.

Based on the results shown, the deviating results for $MgSt_1$ + MCC_{fine}/MCC_{medium} could be explained by scenario 1, indicating an increased shear strength of the applied $MgSt_1$ compared to the other grades. This hypothesis is supported by the fact that $MgSt_1$ is a technical grade of MgSt in contrast to $MgSt_2$ – $MgSt_4$ that resemble pharmaceutical grades. Technical grades with a higher stearate content are known to exhibit higher shear strength [44]. If the coarsest MCC grade with a decreased total surface is applied, the resulting particle size and number of particles after delamination of $MgSt_1$ is sufficient to cover the available MCC surface, similar to the other MgSt grades (Figure 7c).

If Scenario 2 would be valid, for a given lubricant mass the total surface to be covered determines the fraction of surface coverage and by that, the minimal compactibility. As the total surface to be covered is determined by the MCC grade, coarser MCC grades should generally exhibit smaller compactibility values. In fact, a slight tendency for an opposing effect is apparent: coarser MCC grades show slightly higher $\sigma_{0,end}$ values (Figure 8a). It could be hypothesized that larger MCC particles exhibit a greater absolute deformation during compaction, which could result in an increased interference with the lubricant coverage. Additionally, a small degree of fragmentation was identified for coarse MCC grades by Roberts and Rowe [45]. Both mechanisms could result in an increase of fresh, unlubricated surfaces that are available for bonding, which could explain the slightly higher $\sigma_{0,end}$ values of coarser MCC grades. However, though it may prevail during the whole dispersion process, this specific effect can only be differentiated towards $\sigma_{0,end}$ because at lower dispersion states, the higher surface coverages of coarser MCC particles overrule this effect by lower strength compared with smaller MCC particles. This finding in combination with the general similarity of the found $\sigma_{0,end}$ values contradicts scenario 2.

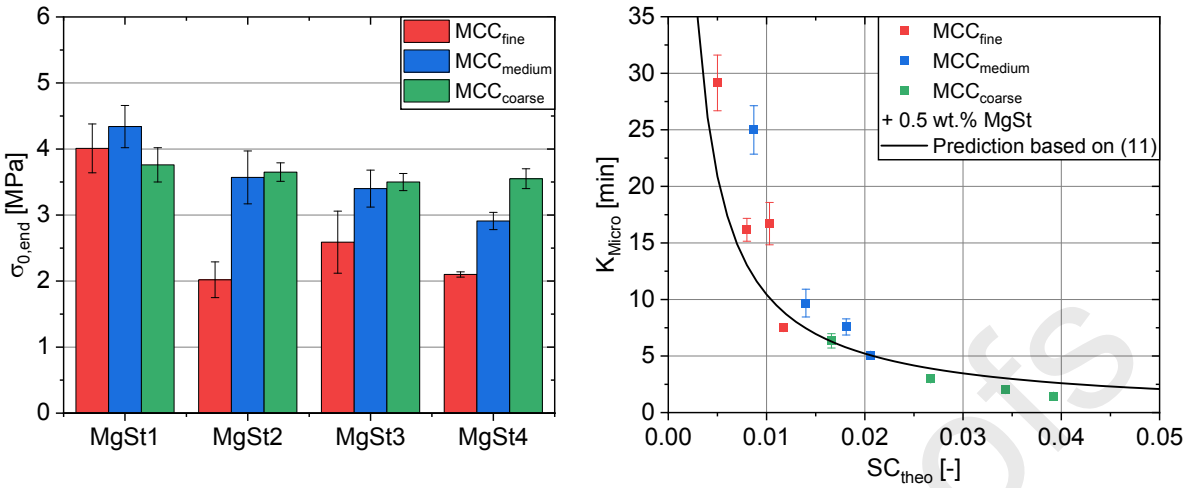

(a) (b)

Figure 8: Derived $\sigma_{0,end}$ (a) and K_{Micro} (b) values by fitting σ_0 vs. t_{mix} plots with equation (10) for different binary combinations of MCC and MgSt grades. Line in (b) represents prediction of K_{Micro} based on equation (11) and K_{Macro} derived of Figure 6d.

Thus, it can be hypothesized that scenario 3 best describes the equilibrium state for the majority of investigated formulations. To check this hypothesis, it was investigated whether the identified common equilibrium state is the consequence of the constant added lubricant mass or refers to the saturation of the majority of available MCC surfaces. Therefore, binary mixtures of all MCC grades and MgSt grades were created by applying a mixing time of 120 min and systematically varying the lubricant concentration between 0.02 – 1 wt.% (for $MgSt_1$ also 2 wt.%) (Figure S3). The mixing time of 120 min was chosen in order to ensure a sufficiently high number of stress events to achieve higher dispersion and to come close to a possible equilibrium while simultaneously keeping the experiments feasible in terms of time.

Afterwards, the compactibility profiles were mathematically quantified by applying the Ryshkewitch-Duckworth equation while assuming that the bonding capacity can be estimated by the bonding capacity of the unlubricated diluent $k_{b,dil}$. The resulting σ_0 values are plotted against the SC_{theo}, which represents the surface coverage of MCC after the macroscopic lubricant dispersion. It is evident, that a common relationship between σ_0 and SC_{theo} irrespective of the applied formulation can be identified (Figure 9**)**.

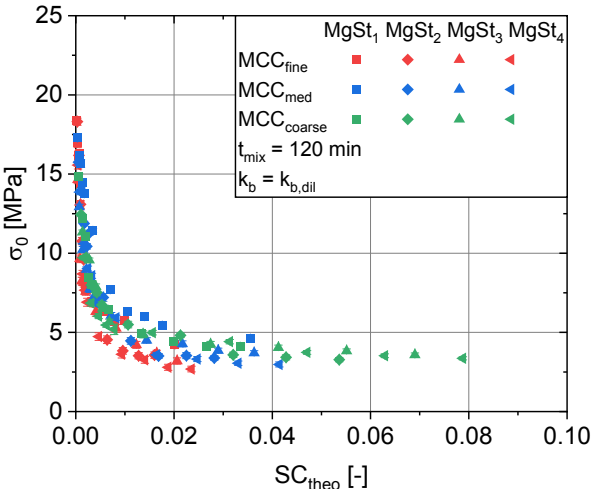

Figure 9: Reduction of σ_0 as a function of SC_{theo} for different binary mixtures of MCC and MgSt for a mixing time of 120 min.

The resulting σ_0 values rapidly decrease between initial SC_{theo} values of 0 – 0.01 and subsequently approach a threshold of σ_0 between 3 – 4 MPa, similar to the results shown in Figure 7. Thereby, if a sufficient amount of lubricant is added to the formulation, a similar equilibrium state of compactibility results. This indicates that this equilibrium describes the residual bonding potential of lubricated MCC surfaces. Interestingly, higher $MgSt_1$ concentrations also results in a comparable minimum σ_0 values. This can be seen as confirmation that the deviating results for $MgSt_1$ + MCC_{fine}/MCC_{medium} is in fact attributed to its enhanced shear strength and does not indicate an entirely different behavior. Generally, the dataset can be divided into a rapid decrease of σ_0 followed by a very slow decrease of σ_0. The transition area is located at SC_{theo} values of 0.01, which can be seen as a minimum value to ensure a common equilibrium state for high mixing times. This correlates to lubricant concentrations between 0.1 wt.% (MCC_{coarse} + $MgSt_4$) and 1 wt.% (MCC_{fine} + $MgSt_1$) and is well within the commonly applied range of pharmaceutical lubricant concentrations. Thus, from a practical point of view, a common minimal compactibility value can be assumed. For SC_{theo} values below 0.01, considerably higher σ_0 values were found. This increased compactibility could either be caused by an insufficient lubricant mass or an insufficient number of stress events. As those small lubricant concentrations are typically not applied, no further laborious experiments with prolonged mixing times were performed.

Thereby, following the stress model for comminution processes by Kwade [46], it can be hypothesized that the complete saturation of available MCC surfaces by MgSt particles can be achieved if the following criteria are met:

1. During mixing, the stress energy during stress events is sufficiently high to enable the lubrication dispersion, i.e. by deagglomeration and delamination.
2. The applied mixing time is sufficiently long in order to ensure a sufficient number of successful stress events, which result in lubricant delamination.
3. The applied lubricant mass is sufficiently high, so that the number and size of generated lubricant particles after delamination is sufficient to cover the available MCC surfaces.

Assuming that the $\sigma_{0,dil}$ values are known and $\sigma_{0,end}$ values can be reasonably estimated, the dispersion behavior is mainly governed by the dispersion rate. The dispersion rate describes the rate of which a given MCC surface is covered by lubricant particles and is quantified by the kinetic constant, K_{Micro}. Here, K_{Micro} represent the necessary mixing time until σ_0 is reduced by 50% of the difference between $\sigma_{0,dil}$ and $\sigma_{0,end}$. Thus, smaller K_{Micro} values represent a fast dispersion rate and vice versa.

Correlating the kinetic constant K_{Micro} to SC_{theo}, which represents the macroscopic lubricant dispersion, reveals a rapid decrease of K_{Micro} for increasing SC_{theo} values (Figure 8b). This relationship can be mechanistically understood as the probability that an individual available MCC surface spot is covered

by MgSt in a given time step. It is envisioned, that the delamination of lubricant particles due to shear stresses acting during mixing occurs if a lubricant particle is stressed between two MCC particles, which effectively act comparable to grinding media [46]. If a higher degree of MCC surface is already covered by lubricant particles after the macroscopic lubricant dispersion, the probability to stress a lubricant particle during a stress event is increased. Thereby, the dispersion rate during MgSt delamination directly depends on the macroscopic dispersion state. It is assumed that the different consecutive realized dispersion states of the investigated formulations are comparable, irrespective of the applied particle sizes (Figure 10). Thus, higher SC_{theo} values can be understood as a headstart, which results in short necessary mixing times, and by that smaller K_{Micro} values, to completely cover the diluent surface.

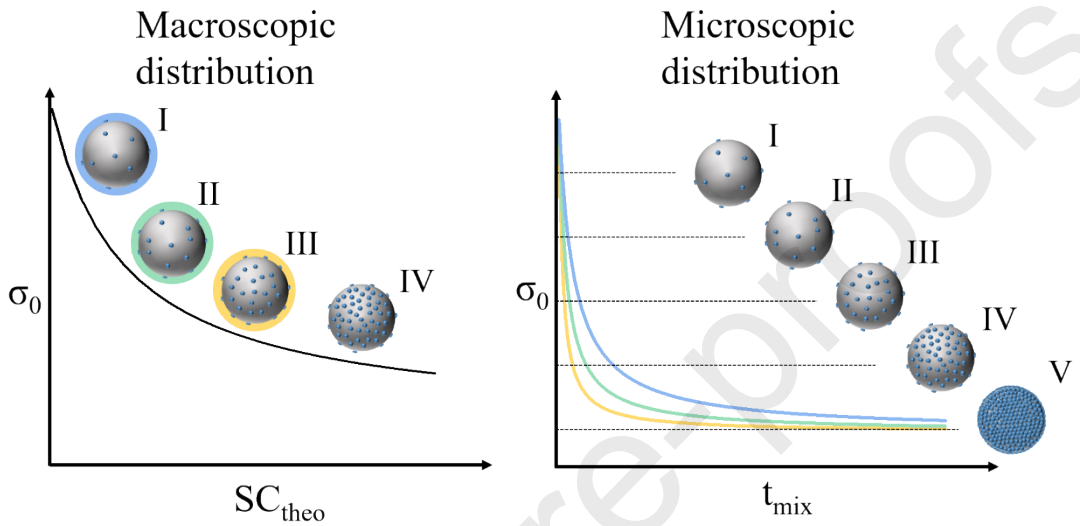

Figure 10: Schematic representation of proposed dispersion states of MgSt as a function of the macroscopic and microscopic lubricant distribution.

Additionally, it can be assumed that the minimal compactibility of lubricated MCC is comparable independent of the type of distribution (be it macroscopic or microscopic) if sufficient amounts of lubricant are applied. Following, $\sigma_{0,dil}$ and $\sigma_{0,end}$ can be estimated to be equal. Assuming that the dispersion kinetics for the influence of concentration and mixing time coincide for a mixing time of 2 min, the dependence of K_{Micro} on SC_{theo} can be determined analytically. Therefore, equation (8) and (10) are equated for t_{mix} = 2 min and solved for K_{Micro}:

$$K_{Micro} = \frac{2\ min \cdot K_{Macro}}{SC_{theo}} \quad (11)$$

Plotting the resulting predicted K_{Micro} values (Figure 8b) showed a correct trend between the predicted and experimental K_{Micro} values. This finding is valuable as it allows the prediction of the dispersion behavior for prolonged mixing times without performing any mixing experiments for prolonged times. Instead, once the impact of lubricant addition on tablet compactibility for a small number of lubricant concentrations is established (c.f. Figure 6d) and modeled by equation (8), the dispersion behavior can already be reasonable predicted.

In summary, the influence of particle size on delamination behavior of MgSt on MCC particles can be divided into two aspects. The minimal compactibility for long mixing times appears to be comparable for the vast majority of investigated formulations with a given MgSt concentration, indicating that this equilibrium state is controlled by the residual bonding strength between lubricated MCC surfaces. The kinetics of dispersion, on the other hand, depend significantly on the set particle size-based surface

coverage due to the macroscopic distribution of MgSt after short mixing times, as it directly affects the probability that a MgSt particle is stressed during MCC particle contact. The findings shown here allow to quantitatively model the particle size influence on the tablet strength of binary mixtures of MCC and MgSt for prolonged mixing times for the first time and by that, can provide a substantial improvement of the available formulation knowledge.

In future studies, it would be desirable to quantify the lubricant particle strength and relating it to stress conditions during relevant pharmaceutical unit operations, e.g. mixing, to further rationalize the lubricant selection. Additionally, as these study has focused on a given set of process parameters, it would be desirable to combine this approach with models which take into account the effect of mixing process parameters on the tablet strength, e.g. the model of Kushner [4]. Finally, an extension of the findings on multi-component mixtures would represent a considerable economic benefit, as it would allow minimizing the number of required experiments.

4. Conclusions

In this study, the influence of the excipient particle size on the compactibility of binary mixtures of MCC and MgSt was investigated using three grades of MCC and four grades of MgSt. The impact of formulation was quantified by estimating the theoretical surface coverage and subsequently, correlated with the reduction of compactibility. Here, the effect of lubricant concentration and mixing time on this correlation was investigated in detail.

It was shown that the compactibility reduction for short mixing times could be modeled independent of the grades used by introducing theoretical surface coverage, which describes the surface coverage of diluents surfaces after the macroscopic lubricant distribution for short mixing times. The theoretical surface coverage requires only easily measurable formulation properties and allows predicting the compactibility reduction if components are replaced by other grades with different particle sizes. In addition, it was shown that, for a sufficient lubricant amount, the minimum compactibility for long mixing times is comparable for the majority of the formulations investigated, if a industrially common low threshold (< 0.5 wt.%) is overcome. This allows to mathematically limit the influence of the lubricant addition on the compactibility for prolonged mixing times to the dispersion rate. It could be shown that this dispersion rate mainly depends on the given theoretical surface coverage, since it determines the probability that a lubricant particle is stressed during an MCC particle contact and, by that, the probability of successful lubricant dispersion events.

Accordingly, the relationships shown in this framework represent a significant improvement in formulation knowledge regarding the linkage of applied excipient sizes on the compactibility reduction of lubricated MCC tablets. This knowledge can be transferred to other formulation components and can be used to streamline the development of new tablet formulations, minimizing the necessary empirical testing. This approach can also be applied directly for granules, which are quite frequently used for tableting. It could even be extended to materials causing too high ejection stresses and tablet defects for the unlubricated case, when external lubrication is applied to assess their compactibility data.

Table of Symbols

d_t	tablet diameter
ε	the tablet porosity
F_B	tablet breaking force

h_t	tablet height
k_b	bonding capacity
K_{Macro}	empirical kinetic constant for macroscopic distribution of lubricant particles
K_{Micro}	empirical kinetic constant for microscopic distribution of lubricant particles
m_t	tablet mass
m_{dil}	total diluent mass
m_{lub}	total lubricant mass
ρ_{tablet}	tablet density
ρ_s	solids density
$S_{m,LD}$	specific surface area determined by laser diffraction
$S_{m,BET}$	specific surface area determined by gas adsorption
S_{dil}	total available diluent surface
S_{lub}	total area occupied by lubricant particles
SC_{theo}	particle size-based theoretical surface coverage
σ_t	tablet tensile strength
σ_0	theoretical maximal tensile strength for a non-porous tablet
$\sigma_{0,lub}$	σ_0 of lubricated formulations
$\sigma_{0,dil}$	σ_0 of pure diluents
$\sigma_{0,norm}$	$\sigma_{0,lub}$ normalized to $\sigma_{0,dil}$

$\sigma_{0,end}$	asymptotic value of σ_0 for high blending times
$\sigma_{0,end,norm}$	$\sigma_{0,end}$ normalized to $\sigma_{0,dil}$
t_{mix}	blending time
$x_{50,lub}$	median particle size of the lubricant

References

[1] P.J. Jarosz, E.L. Parrott, Effect of Lubricants on Tensile Strengths of Tablets, Drug Dev. Ind. Pharm. 10 (1984) 259–273. https://doi.org/10.3109/03639048409064649.

[2] J. Bossert, A. Stains, Effect of Mixing on the Lubrication of Crystalline Lactose by Magnesium Stearate, Drug Dev. Ind. Pharm. 6 (1980) 573–589. https://doi.org/10.3109/03639048009065316.

[3] C.K. Bolhuis, C.F. Lerk, P. Broersma, Mixing Action and Evaluation of Tablet Lubricants in Direct Compression, Drug Dev. Ind. Pharm. 6 (1980) 15–33. https://doi.org/10.3109/03639048009051924.

[4] J. Kushner, F. Moore, Scale-up model describing the impact of lubrication on tablet tensile strength, Int. J. Pharm. 399 (2010) 19–30. https://doi.org/10.1016/j.ijpharm.2010.07.033.

[5] A.C. Shah, A.R. Mlodozeniec, Mechanism of surface lubrication: influence of duration of lubricant-excipient mixing on processing characteristics of powders and properties of compressed tablets, Journal of Pharmaceutical Sciences 66 (1977) 1377–1378. https://doi.org/10.1002/jps.2600661006.

[6] L. Roblot-Treupel, F. Puisieux, Distribution of magnesium stearate on the surface of lubricated particles, Int. J. Pharm. 31 (1986) 131–136. https://doi.org/10.1016/0378-5173(86)90222-X.

[7] A. Skelbæk-Pedersen, T. Vilhelmsen, V. Wallaert, J. Rantanen, Quantification of Fragmentation of Pharmaceutical Materials After Tableting, Journal of Pharmaceutical Sciences 108 (2019) 1246–1253. https://doi.org/10.1016/j.xphs.2018.10.040.

[8] V. Busignies, B. Leclerc, S. Truchon, P. Tchoreloff, Changes in the specific surface area of tablets composed of pharmaceutical materials with various deformation behaviors, Drug Dev. Ind. Pharm. 37 (2011) 225–233. https://doi.org/10.3109/03639045.2010.504925.

[9] A.H. de Boer, G.K. Bolhuis, C.F. Lerk, Bonding Characteristics by Scanning Electron Miscroscopy of Powders Mixed with Magnesium Stearate, Powder Technology 20 (1978) 75–82.

[10] G.K. Bolhuis, C.F. Lerk, H.T. Zulstra, A.H. de Boer, Film Formation by Magnesium Stearate during Mixin g and Its Effect on Tabletting, Pharmaceutisch Weekblad 110 (1975) 317–325.

[11] K.G. Pitt, M.G. Heasley, Determination of the tensile strength of elongated tablets, Powder Technology 238 (2013) 169–175. https://doi.org/10.1016/j.powtec.2011.12.060.

[12] M. Hussain, P. York, P. Timmins, A study of the formation of magnesium stearate film on sodium chloride using energy-dispersive X-ray analysis, Int. J. Pharm. 42 (1988) 89–95. https://doi.org/10.1016/0378-5173(88)90164-0.

[13] J.-I. Kikuta, N. Kitamori, Effect of Mixing Time on the Lubricating Properties of Magnesium Stearate and the Final Characteristics of the Compressed Tablets, Drug Dev. Ind. Pharm. 20 (1994) 343–355. https://doi.org/10.3109/03639049409050187.

[14] Ragnarsson, G., Hölzer, A. W., Sjögren, J., The influence of mixing time and colloidal silica on the lubricating properties of magnesium stearate, Int. J. Pharm. 3 (1979) 127–131. https://doi.org/10.1016/0378-5173(79)90074-7.

[15] C.A. Gunawardana, A. Kong, D.O. Blackwood, C. Travis Powell, J.F. Krzyzaniak, M.C. Thomas, C. Calvin Sun, Magnesium stearate surface coverage on tablets and drug crystals: Insights from SEM-EDS elemental mapping, Int. J. Pharm. 630 (2023) 122422. https://doi.org/10.1016/j.ijpharm.2022.122422.

[16] M. Hussain, P. York, P. Timmins, P. Humphrey, Secondary Ion Mass Spectrometry (SIMS) Evaluation of Magnesium Stearate Distribution and its Effects on the Physico-Technical Properties of Sodium Chloride Tablets, Powder Technology 60 (1990) 39–45.

[17] S. Lakio, B. Vajna, I. Farkas, H. Salokangas, G. Marosi, J. Yliruusi, Challenges in detecting magnesium stearate distribution in tablets, AAPS PharmSciTech 14 (2013) 435–444. https://doi.org/10.1208/s12249-013-9927-3.

[18] C. de Backere, J. Quodbach, T. de Beer, C. Vervaet, V. Vanhoorne, Impact of alternative lubricants on process and tablet quality for direct compression, Int. J. Pharm. 624 (2022) 122012. https://doi.org/10.1016/j.ijpharm.2022.122012.

[19] D. Puckhaber, J.H. Finke, A. Kwade, Investigation of the dispersion kinetics of particulate lubricants and their effect on the mechanical strength of MCC tablets, Pharm. Res. (2023). https://doi.org/10.1007/s11095-023-03602-0

[20] S. Paul, C.C. Sun, Systematic evaluation of common lubricants for optimal use in tablet formulation, Eur. J. Pharm. Sci. 117 (2018) 118–127. https://doi.org/10.1016/j.ejps.2018.02.013.

[21] J. Barra, R. Somma, Influence of the Physicochemical Variability of Magnesium Stearate on Its Lubricant Properties: Possible Solutions, Drug Dev. Ind. Pharm. 22 (1996) 1105–1120. https://doi.org/10.3109/03639049609065947.

[22] G.K. Bolhuis, S.W. de Jong, C.F. Lerk, H. Dettmers, B.V. Pharbita, The Effect of Magnesium Stearate Admixing in Different Types of Laboratory and Industrial Mixers on Tablet Crushing Strength, Drug Dev. Ind. Pharm. 13 (1987) 1547–1567. https://doi.org/10.3109/03639048709068680.

[23] D. Puckhaber, A. Kathrin Schomberg, A. Kwade, J. Henrik Finke, A compactibility-based lubricant dispersion model describing the effect of formulation and paddle speed, Int. J. Pharm. 628 (2022) 122300. https://doi.org/10.1016/j.ijpharm.2022.122300.

[24] A.S. Narang, V.M. Rao, H. Guo, J. Lu, D.S. Desai, Effect of force feeder on tablet strength during compression, Int. J. Pharm. 401 (2010) 7–15. https://doi.org/10.1016/j.ijpharm.2010.08.027.

[25] I. Wünsch, I. Friesen, D. Puckhaber, T. Schlegel, J.H. Finke, Scaling Tableting Processes from Compaction Simulator to Rotary Presses-Mind the Sub-Processes, Pharmaceutics 12 (2020). https://doi.org/10.3390/pharmaceutics12040310.

[26] J. Kushner, H. Schlack, Commercial scale validation of a process scale-up model for lubricant blending of pharmaceutical powders, Int. J. Pharm. 475 (2014) 147–155. https://doi.org/10.1016/j.ijpharm.2014.08.036.

[27] J. Kushner, Incorporating Turbula mixers into a blending scale-up model for evaluating the effect of magnesium stearate on tablet tensile strength and bulk specific volume, Int. J. Pharm. 429 (2012) 1–11. https://doi.org/10.1016/j.ijpharm.2012.02.040.

[28] D. Puckhaber, J.H. Finke, S. David, M. Serratoni, U. Zafar, E. John, M. Juhnke, A. Kwade, Prediction of the impact of lubrication on tablet compactibility, Int. J. Pharm. 617 (2022) 121557. https://doi.org/10.1016/j.ijpharm.2022.121557.

[29] G.K. Reynolds, J.I. Campbell, R.J. Roberts, A compressibility based model for predicting the tensile strength of directly compressed pharmaceutical powder mixtures, Int. J. Pharm. 531 (2017) 215–224. https://doi.org/10.1016/j.ijpharm.2017.08.075.

[30] D. Puckhaber, A.-L. Voges, S. Rane, S. David, B. Gururajan, J. Henrik Finke, A. Kwade, Enhanced multi-component model to consider the lubricant effect on compressibility and compactibility, Eur. J. Pharm. Biopharm. (2023). https://doi.org/10.1016/j.ejpb.2023.04.004.

[31] C. Schilde, I. Kampen, A. Kwade, Dispersion kinetics of nano-sized particles for different dispersing machines, Chemical Engineering Science 65 (2010) 3518–3527. https://doi.org/10.1016/j.ces.2010.02.043.

[32] J.T. Fell, J.M. Newton, Determination of tablet strength by the diametral-compression test, Journal of Pharmaceutical Sciences 59 (1970) 688–691.

[33] M. Badal Tejedor, N. Nordgren, M. Schuleit, M.W. Rutland, A. Millqvist-Fureby, Tablet mechanics depend on nano and micro scale adhesion, lubrication and structure, Int. J. Pharm. 486 (2015) 315–323. https://doi.org/10.1016/j.ijpharm.2015.03.049.

[34] C.K. Tye, C.C. Sun, G.E. Amidon, Evaluation of the effects of tableting speed on the relationships between compaction pressure, tablet tensile strength, and tablet solid fraction, Journal of Pharmaceutical Sciences 94 (2005) 465–472. https://doi.org/10.1002/jps.20262.

[35] H. Rumpf, Zur Theorie der Zugfestigkeit von Agglomeraten bei Kraftübertragung an Kontaktpunkten, Chemie Ingenieur Technik 42 (1970) 538–540.

[36] L.L. Augsburger, S.W. Hoag, Pharmaceutical dosage forms: Tablets, thirdrd ed., Informa Healthcare, New York, London, 2008.

[37] G.E. Reier, R.F. Shangraw, Microcrystalline Cellulose in Tableting, Journal of Pharmaceutical Sciences 55 (1966) 510–514. https://doi.org/10.1002/jps.2600550513.

[38] K. Zuurman, K. van der Voort Maarschalk, G.K. Bolhuis, Effect of Magnesium Stearate on Bonding and Porosity Expansion of Tablets Produced from Materials with Different Consolidation Properties, Int. J. Pharm. 179 (1999) 107–115.

[39] J. Dun, H. Chen, C.C. Sun, Profound tabletability deterioration of microcrystalline cellulose by magnesium stearate, Int. J. Pharm. 590 (2020) 119927. https://doi.org/10.1016/j.ijpharm.2020.119927.

[40] E. Ryshkewitch, Compression Strength of Porous Sintered Alumina and Zirconia, Journal of the American Ceramic Society 36 (1953) 65–68.

[41] W. Duckworth, Discussion of Ryshkewitch paper, Journal of the American Ceramic Society 36 (1953). https://doi.org/10.1111/jace.1953.36.issue-2.

[42] R. Dansereau, G.E. Peck, The Effect of the Variability in the Physical and Chemical Properties of Magnesium Stearate on the Properties of Compressed Tablets, Drug Dev. Ind. Pharm. 13 (1987) 975–999. https://doi.org/10.3109/03639048709068365.

[43] K. Meyer, Nanomaterialien als Fließregulierungsmittel, Dissertation, Würzburg, 2003.

[44] S.B. Marwaha, M.H. Rubinstein, Structure-lubricity evaluation of magnesium stearate, Int. J. Pharm. 43 (1988) 249–255.

[45] R.J. Roberts, R.C. Rowe, The effect of the relationship between punch velocity and particle size on the compaction behaviour of materials with varying deformation mechanisms, J. Pharm. Pharmacol. 38 (1986) 567–571.

[46] A. Kwade, Wet comminution in stirred media mills - research and its practical application, Powder Technology 105 (1999) 14–20.

Daniel Puckhaber: Conceptualization, Methodology, Validation, Formal analysis, Investigation, Writing – Original Draft, Writing – Review & Editing, Visualization

Jan Henrik Finke: Conceptualization, Methodology, Validation, Formal analysis, Investigation, Writing – Review & Editing, Visualization

Sarah David: Investigation, Writing – Review & Editing

Bindhumadhavan Gururajan: Investigation, Writing – Review & Editing

Supriya Rane: Project administration, Resources

Arno Kwade: Conceptualization, Investigation, Resources, Writing – Review & Editing, Supervision, Project administration

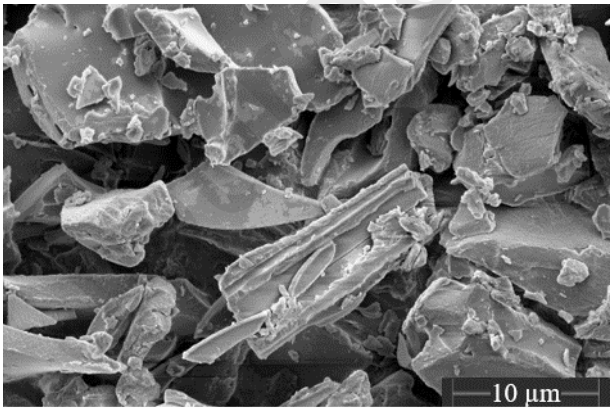

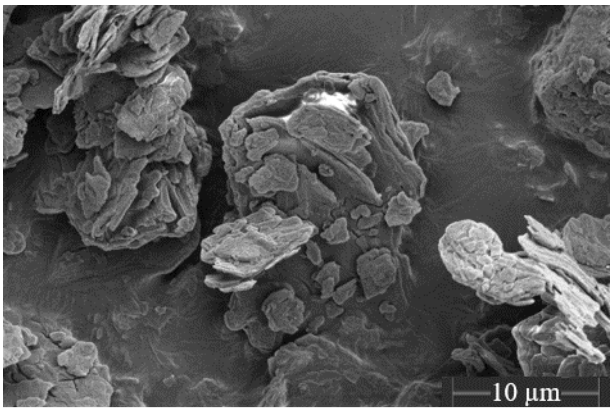

610

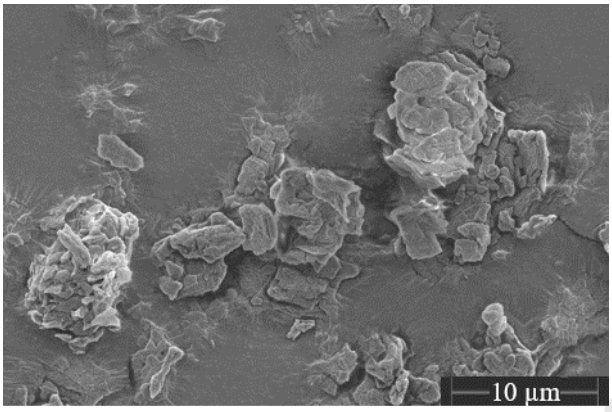

611

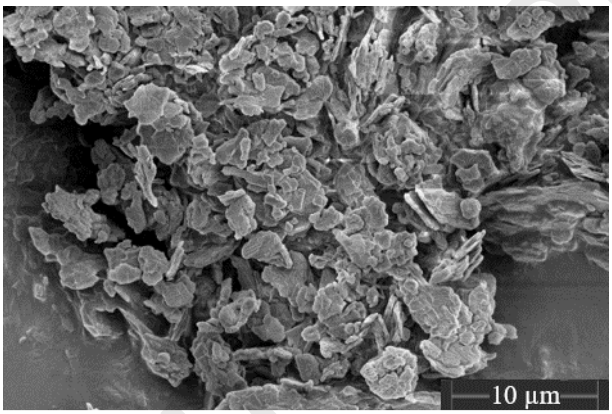

612

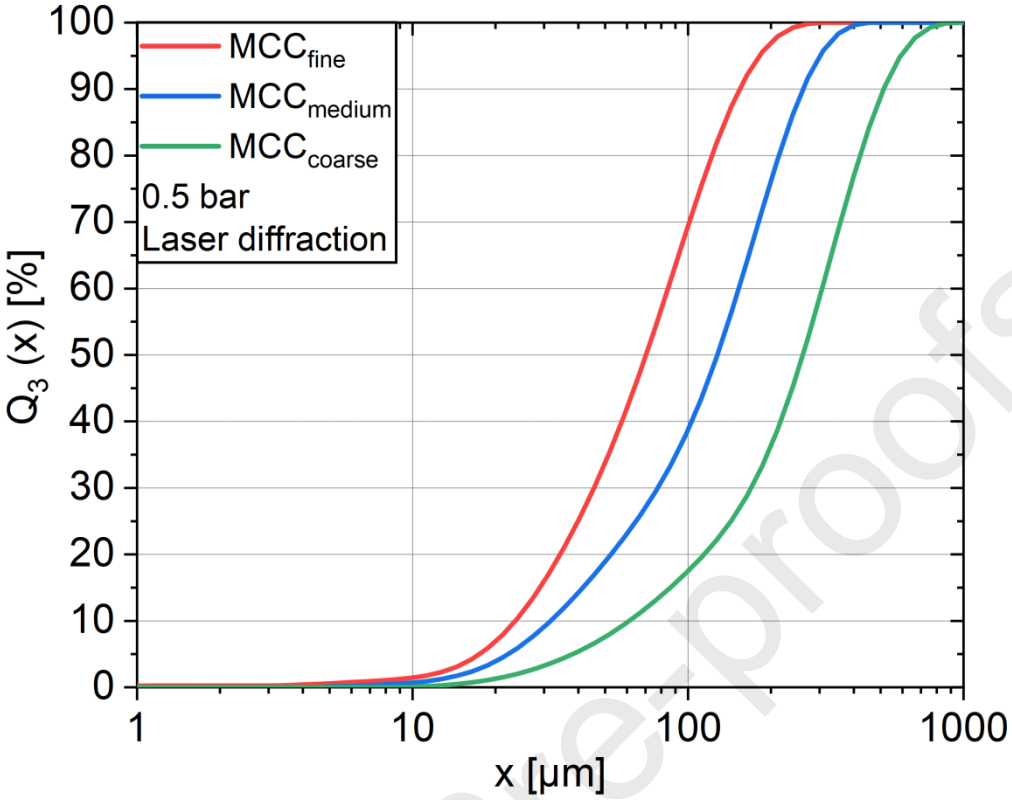

613

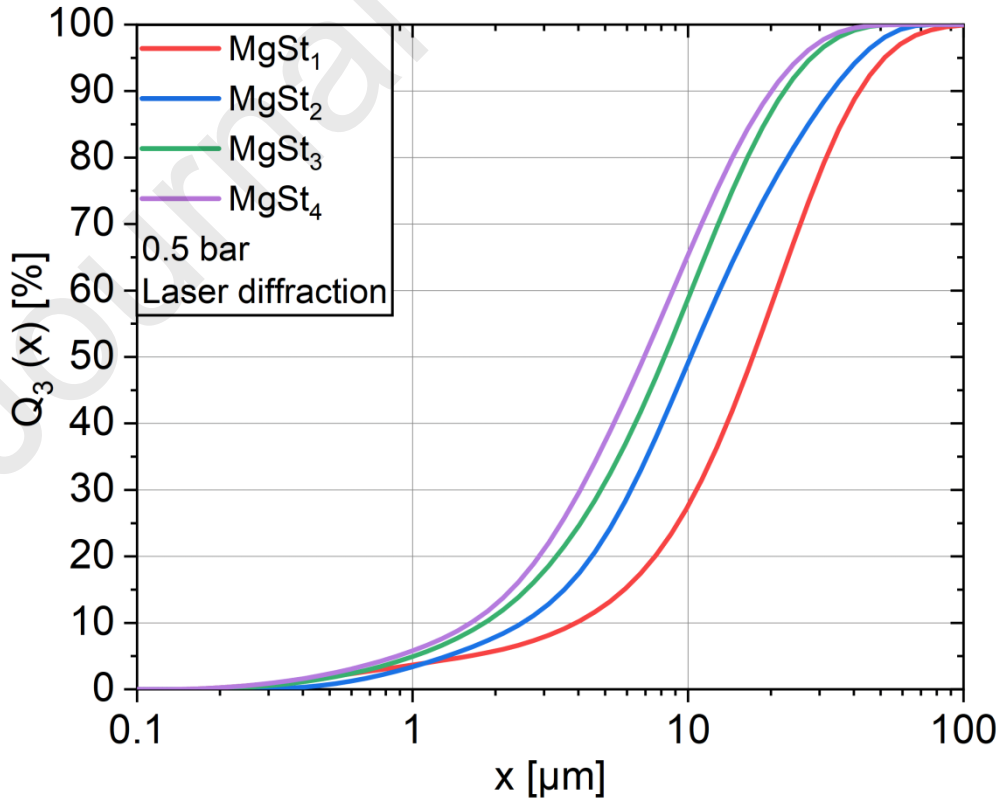

614

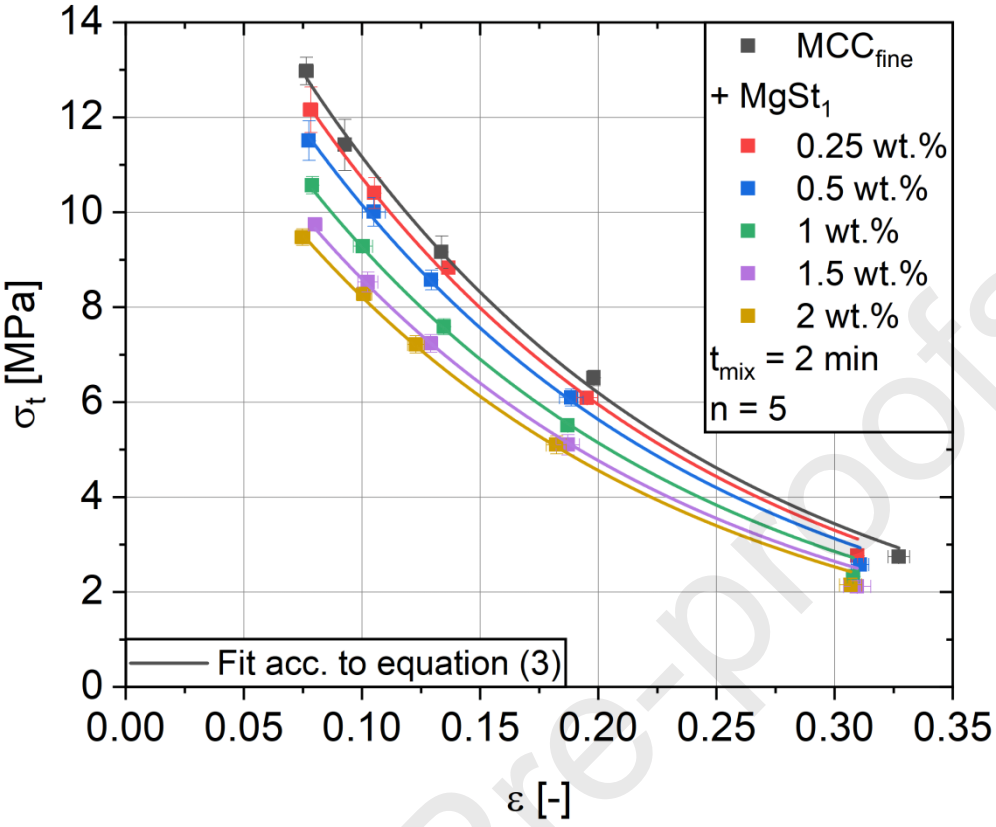

615

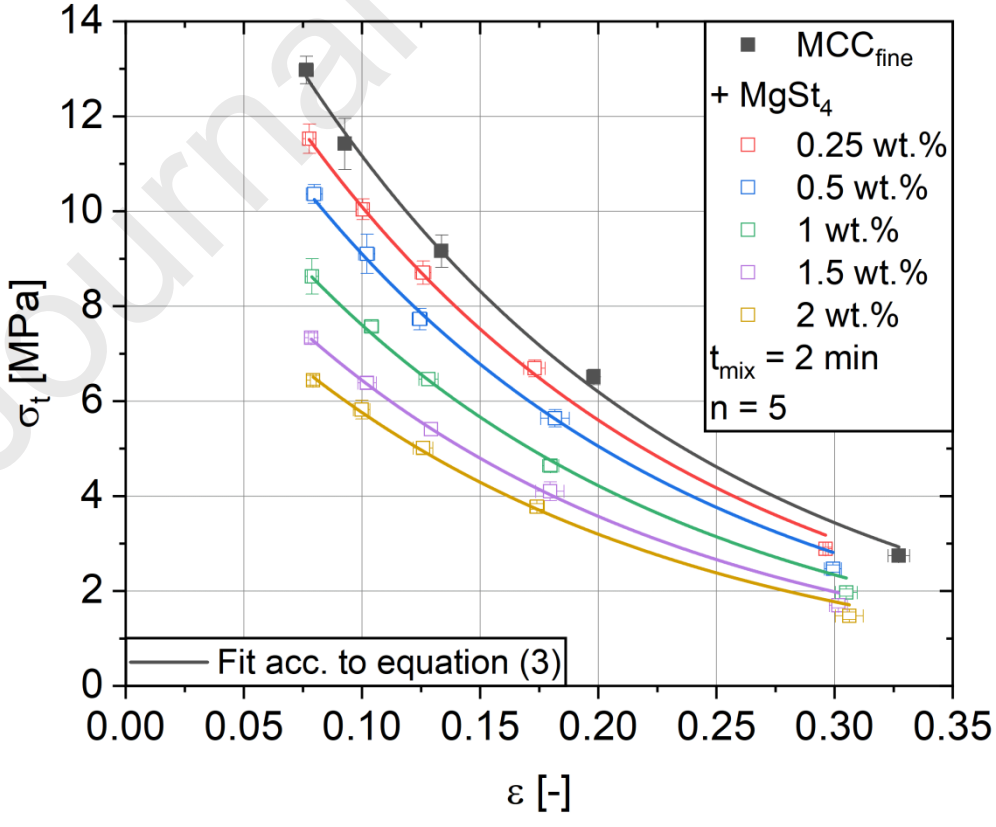

616

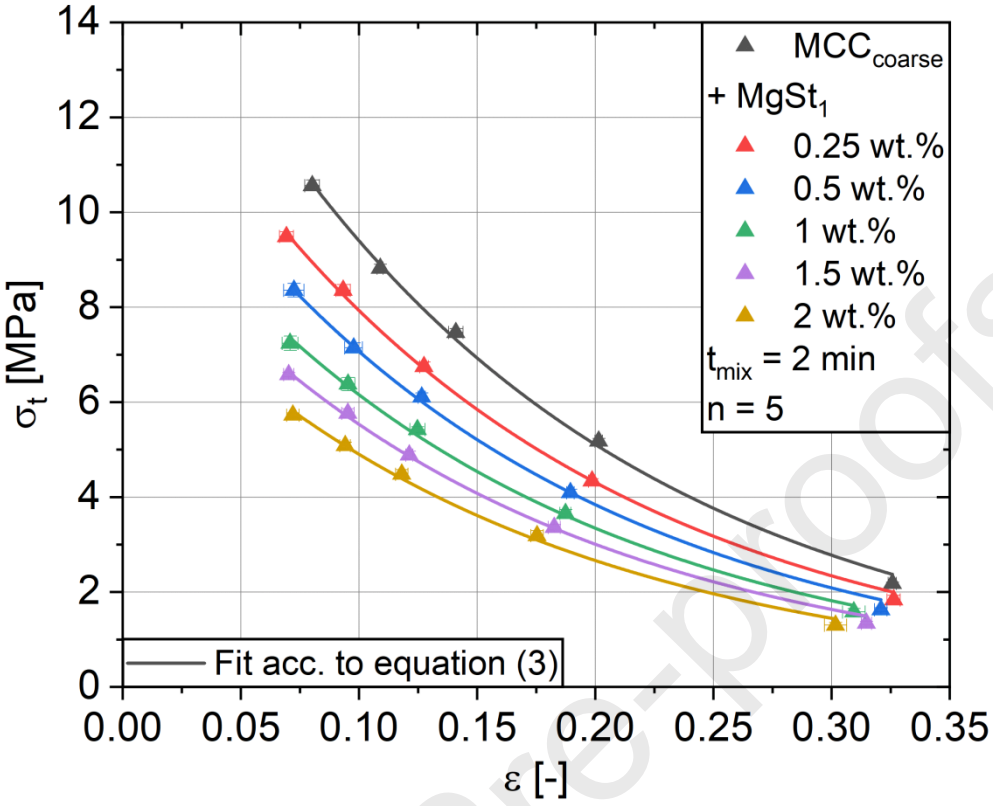

617

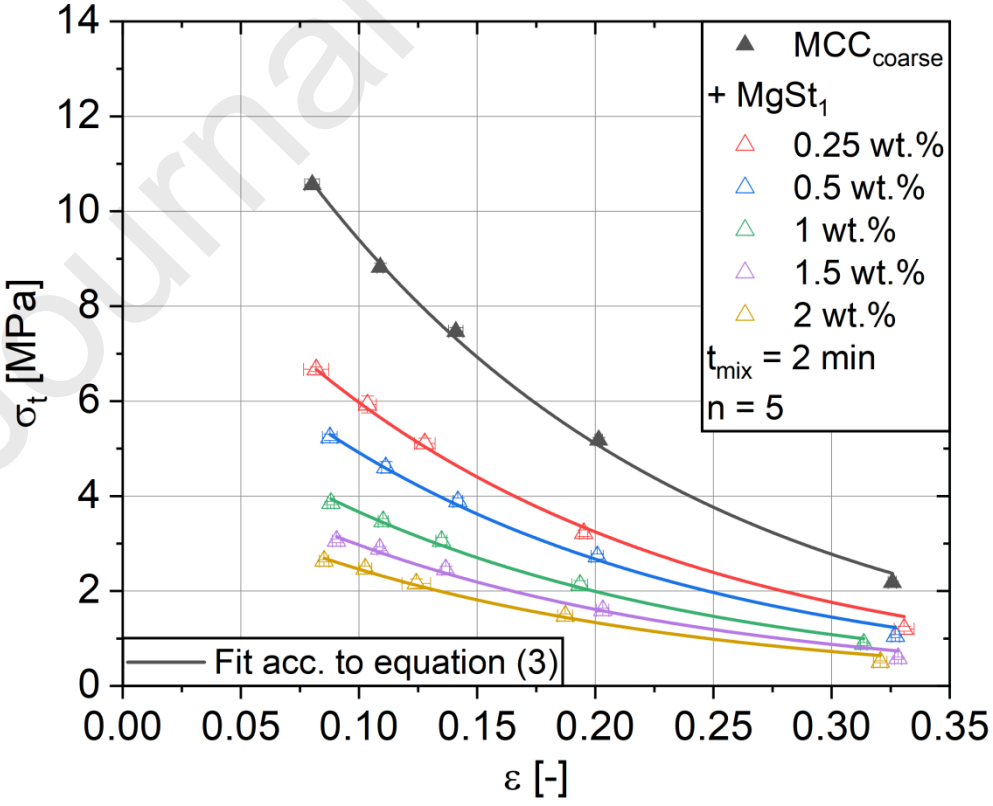

618

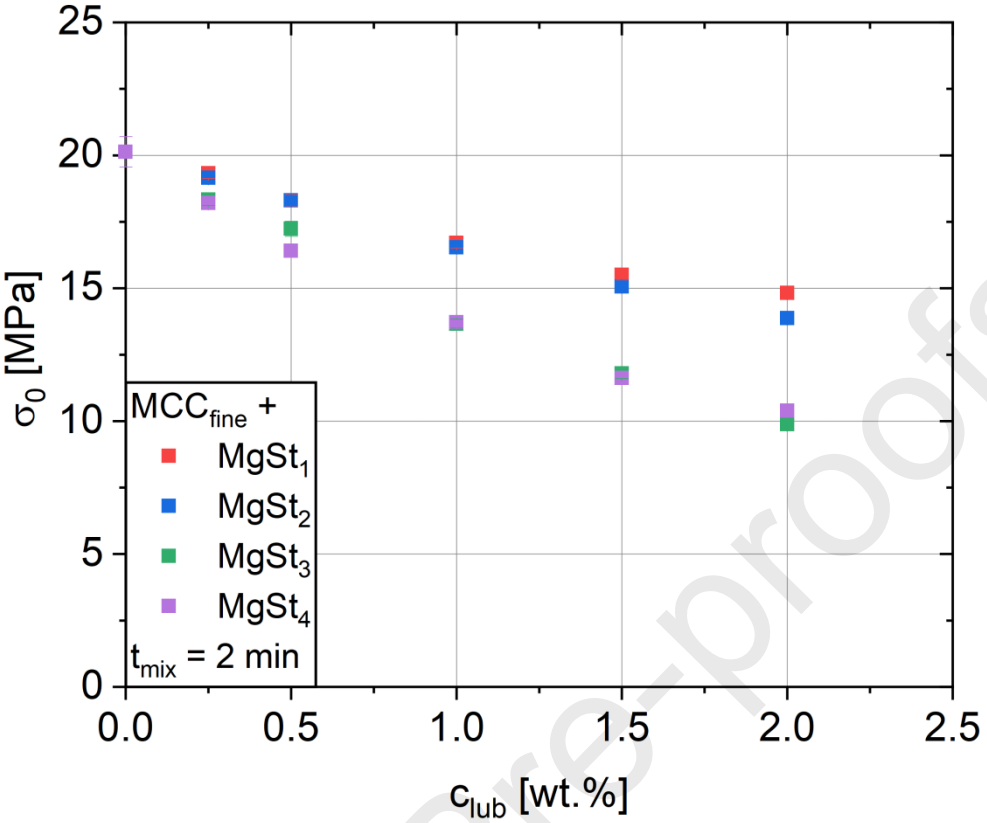

619

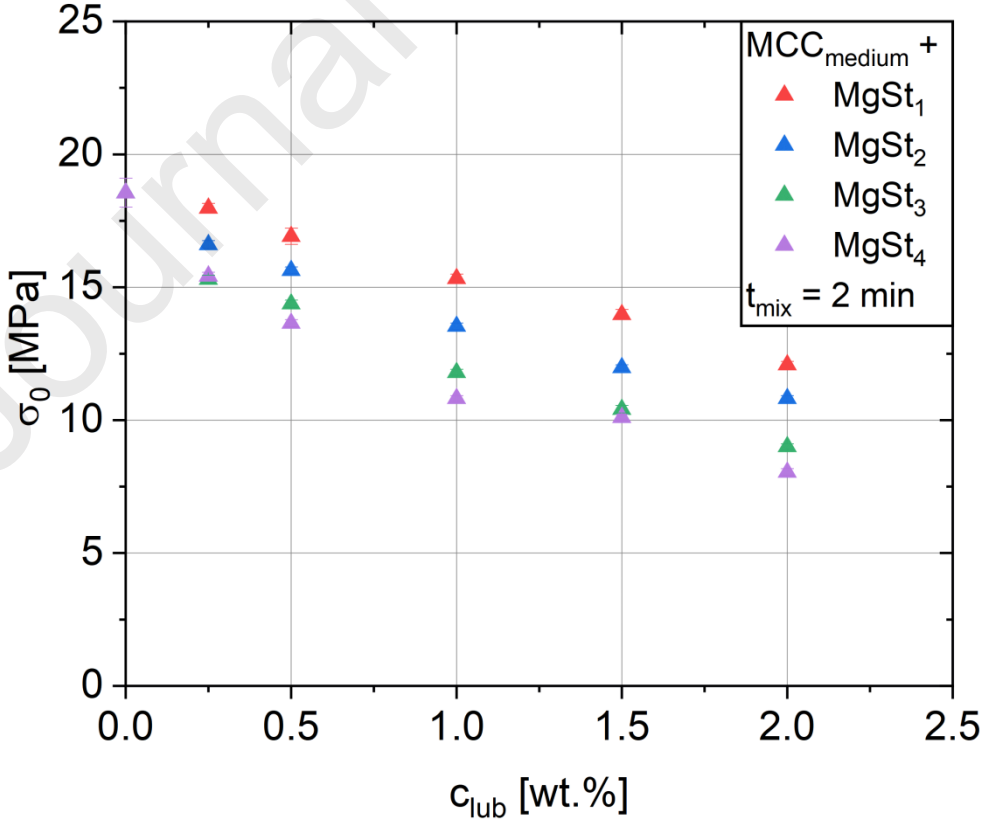

620

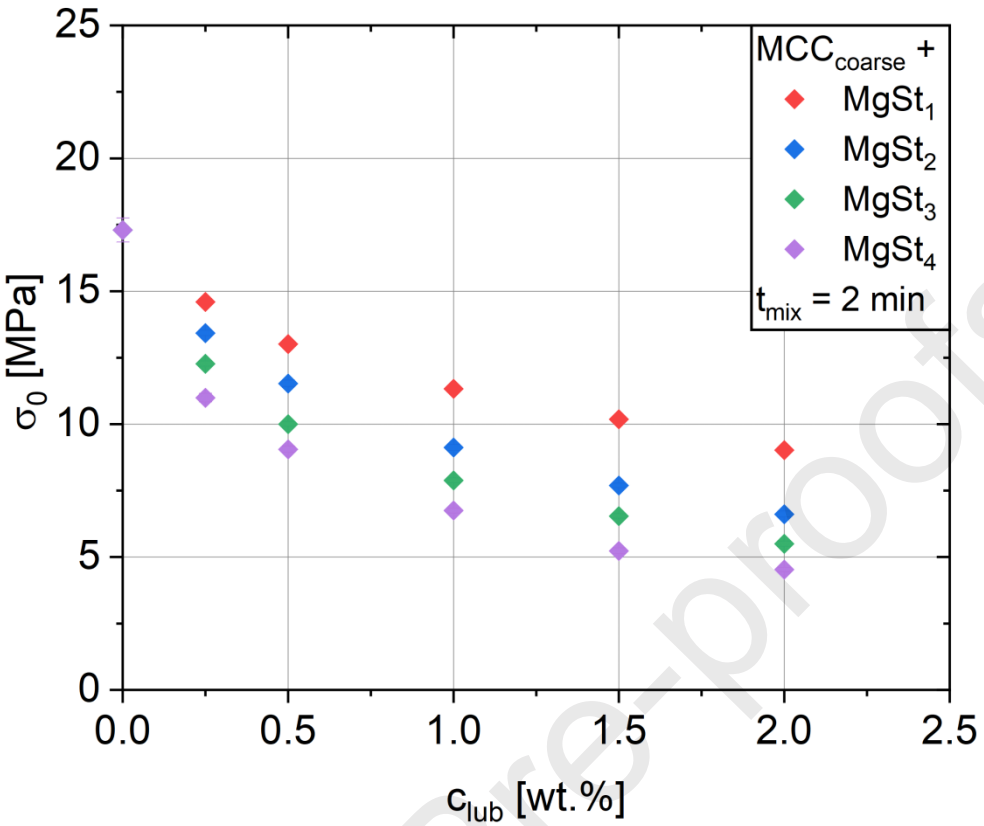

621

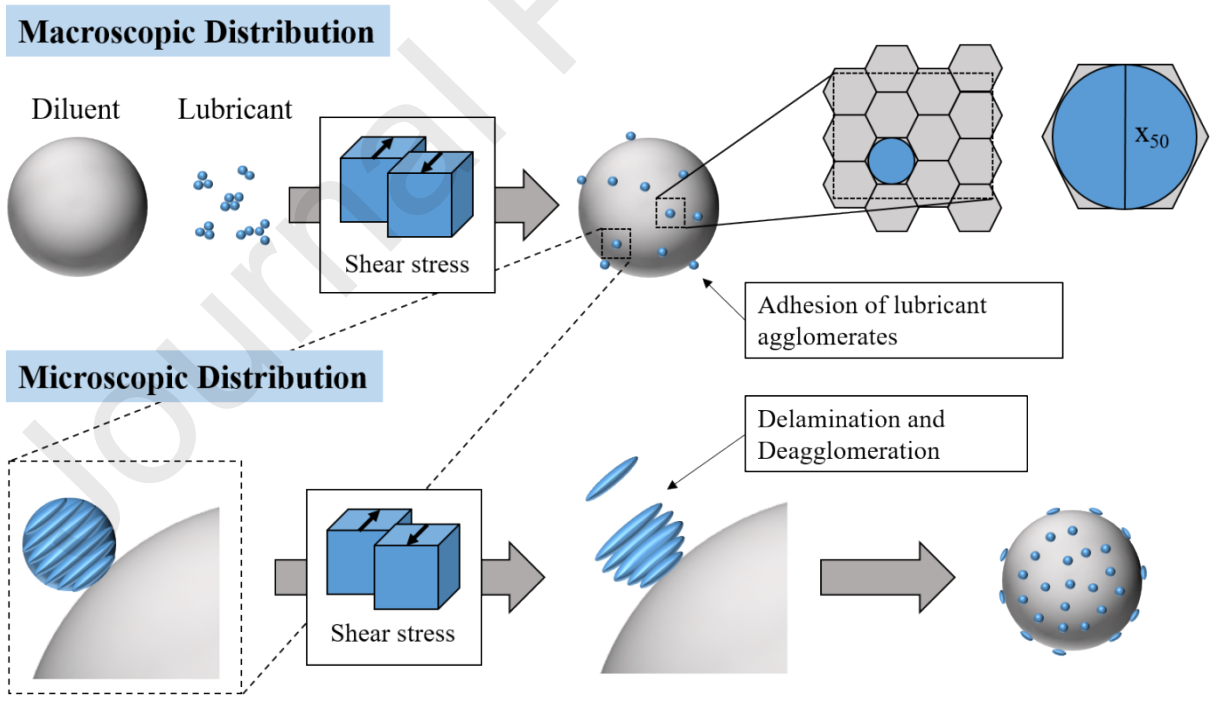

622

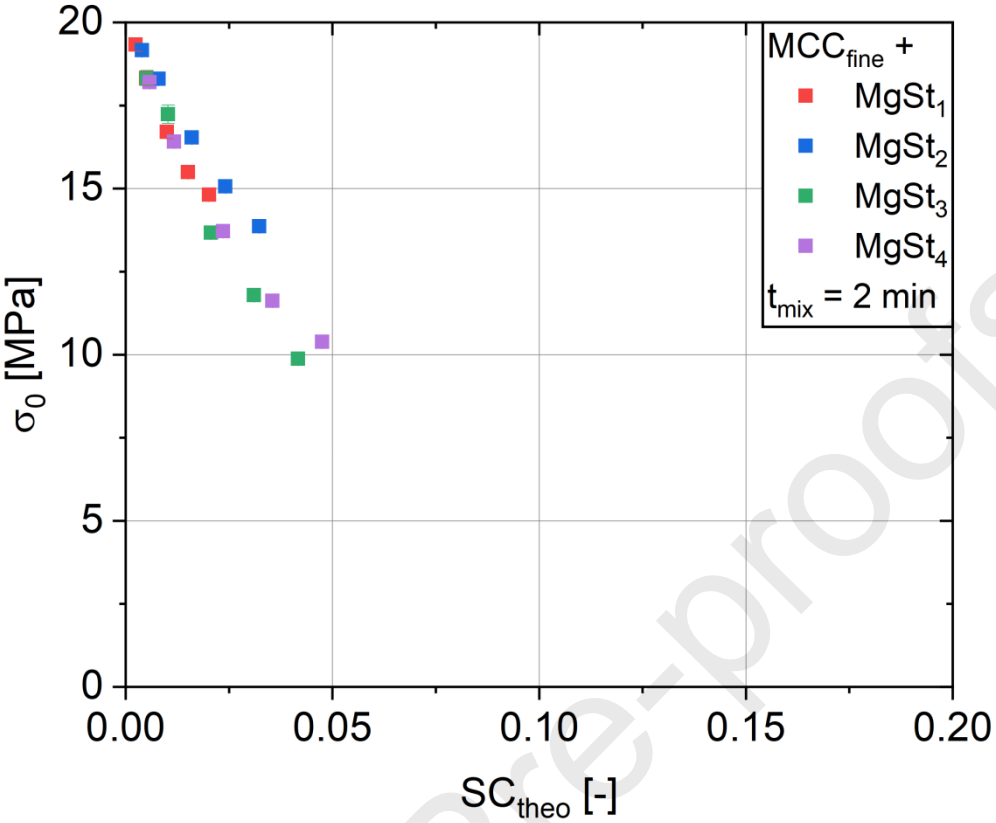

623

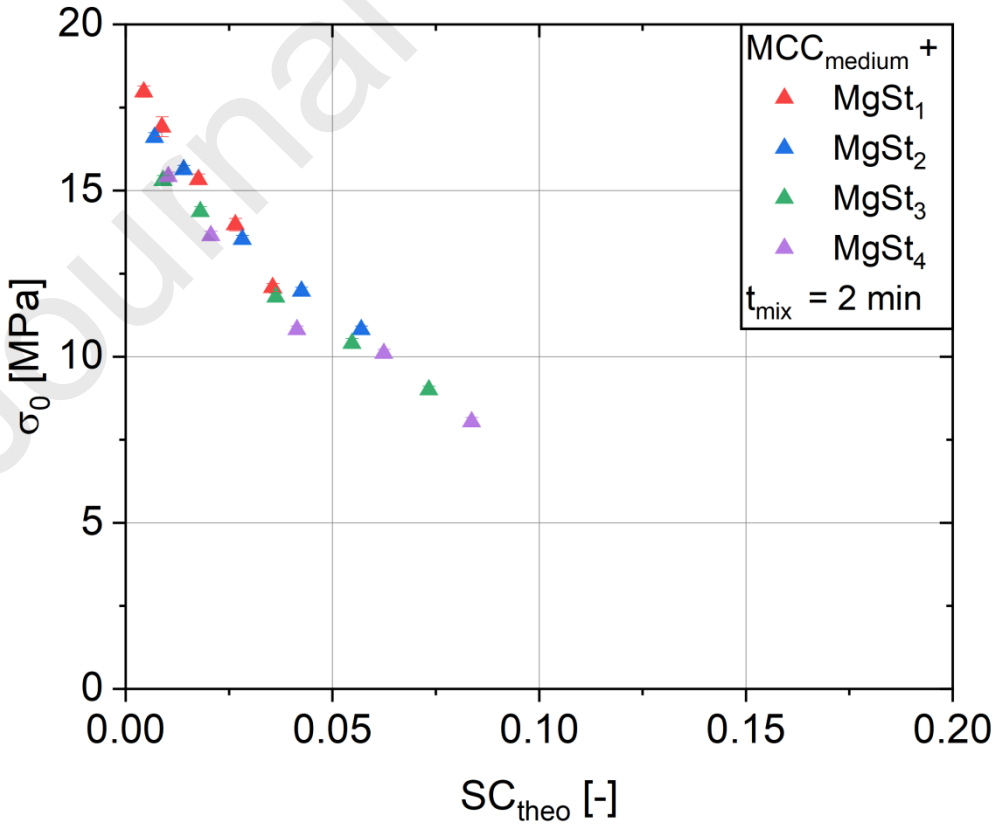

624

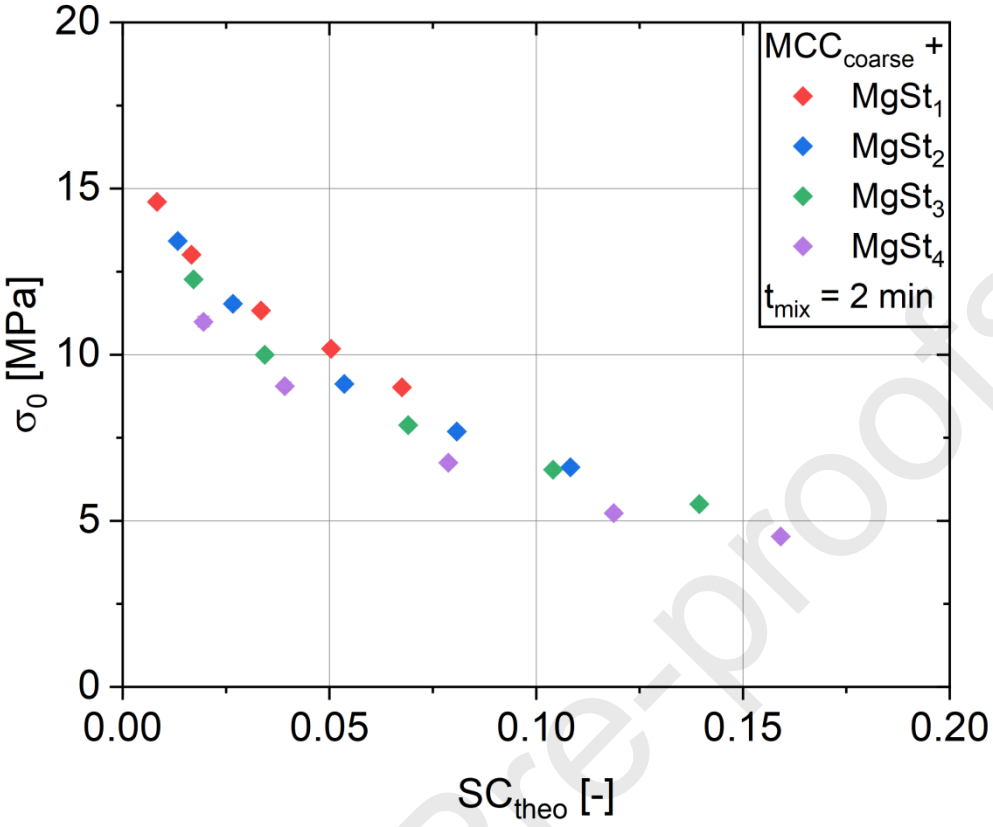

625

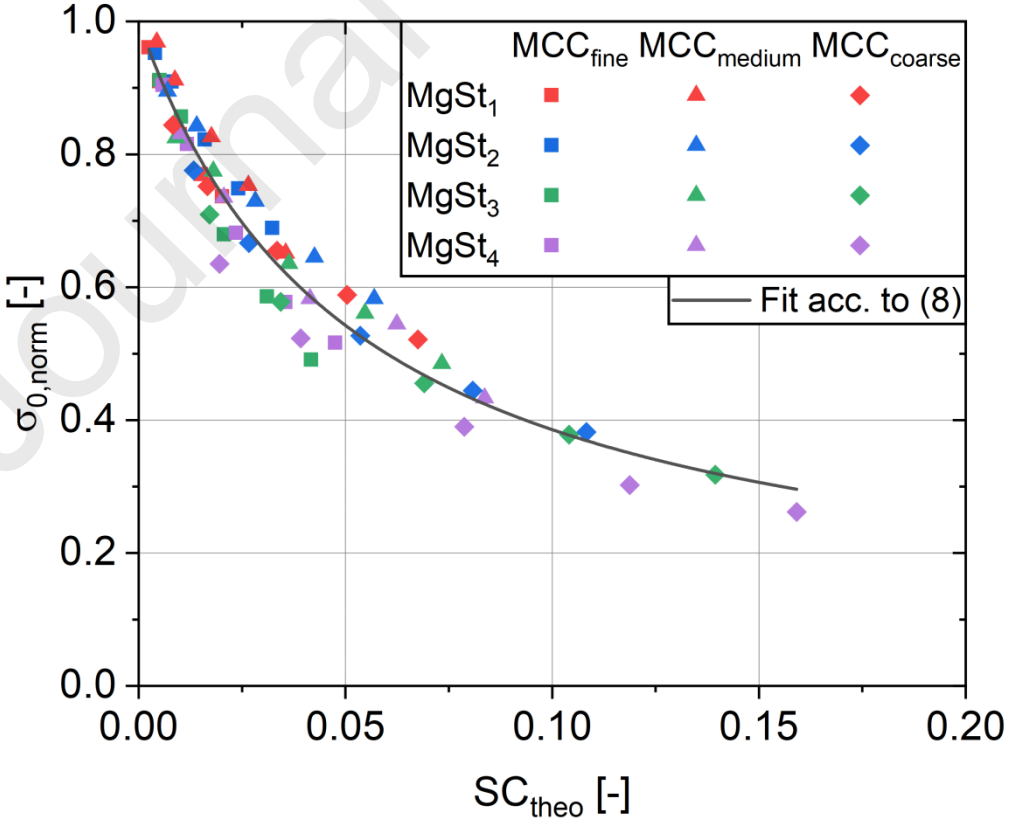

626

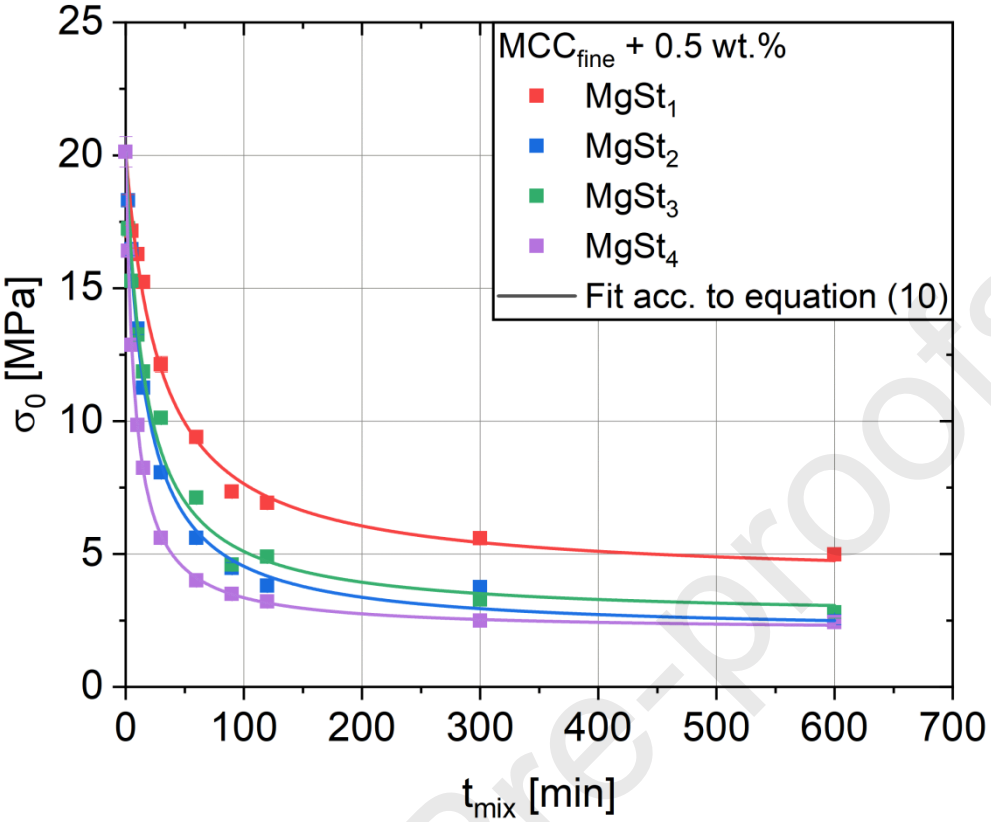

627

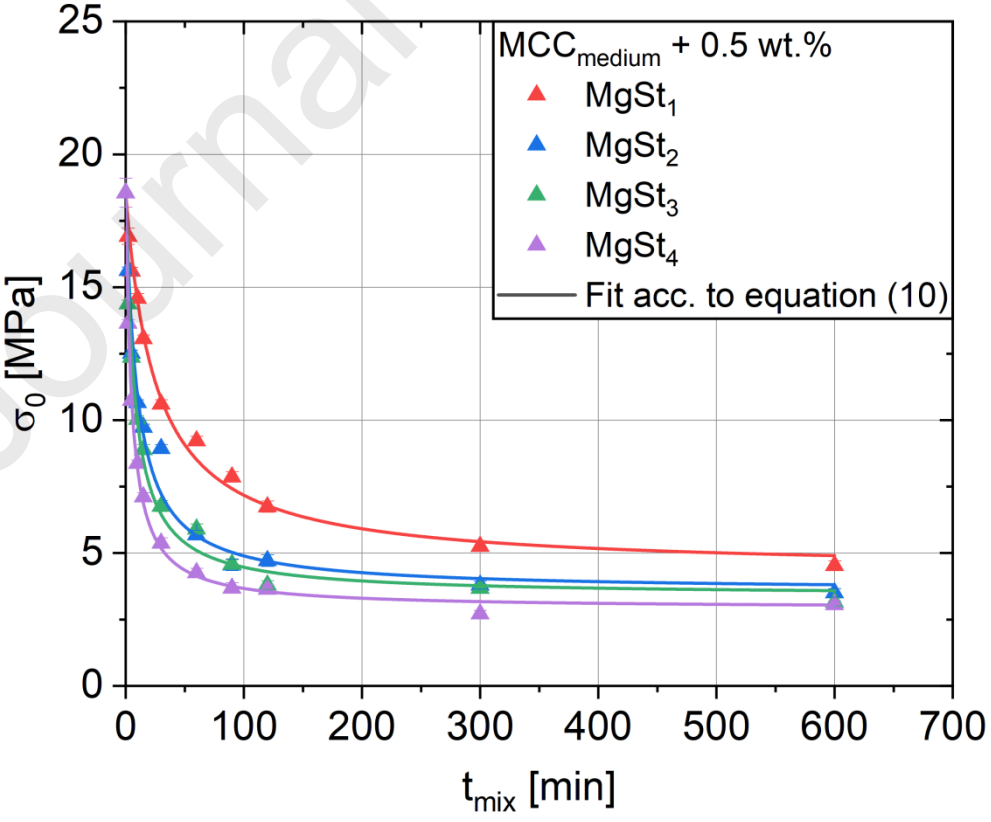

628

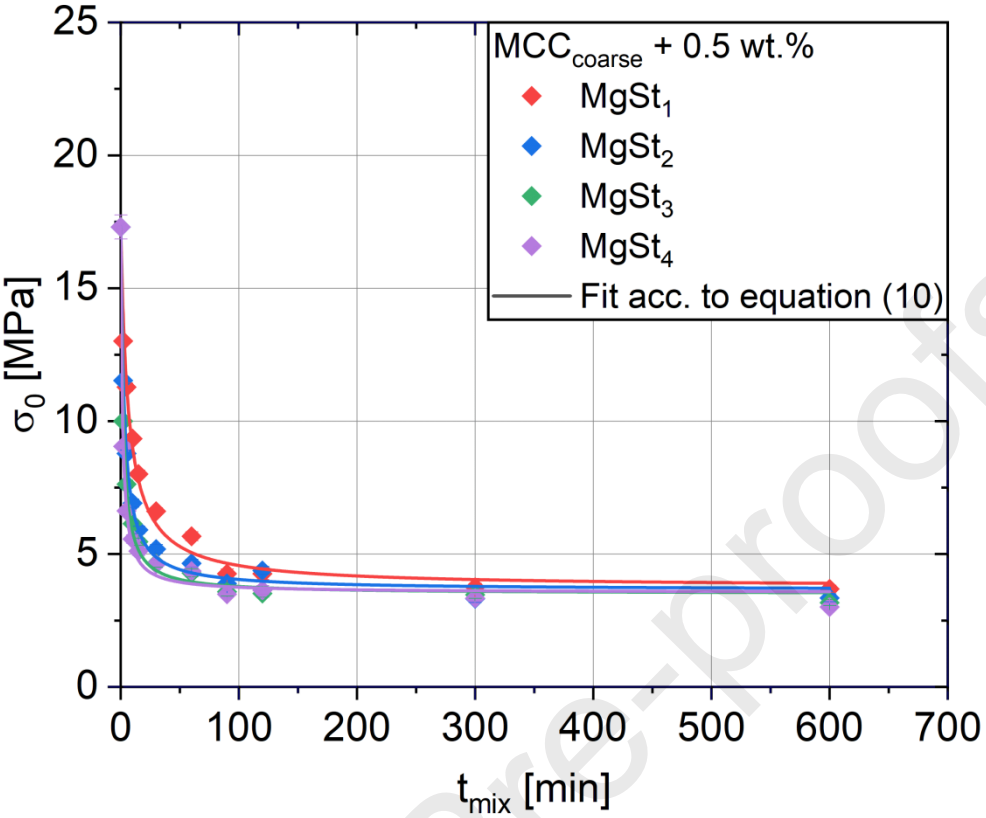

629

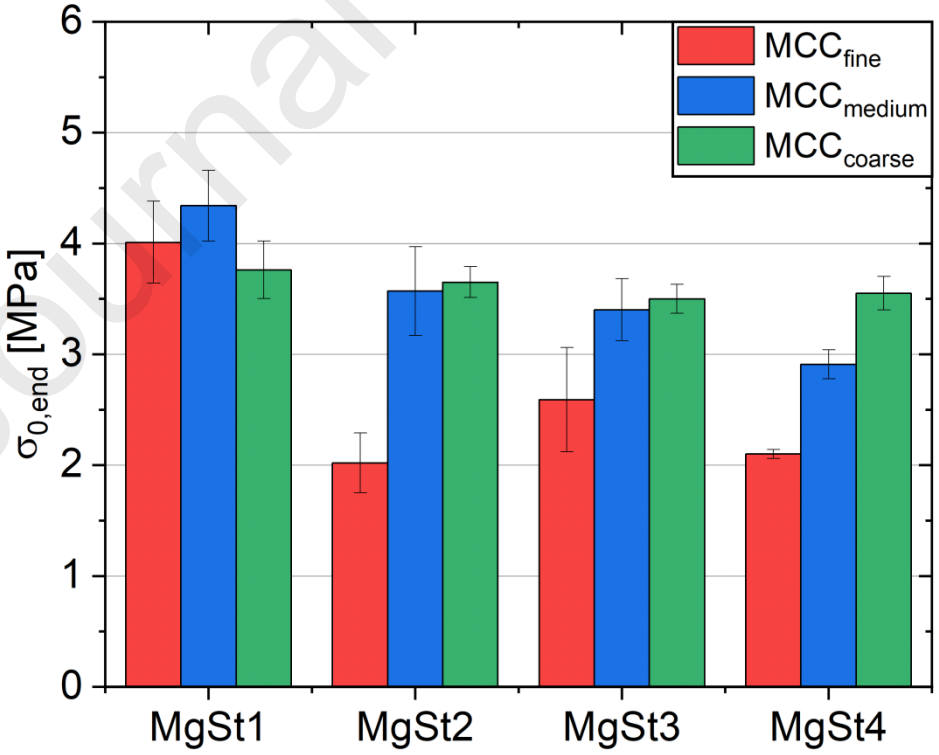

630

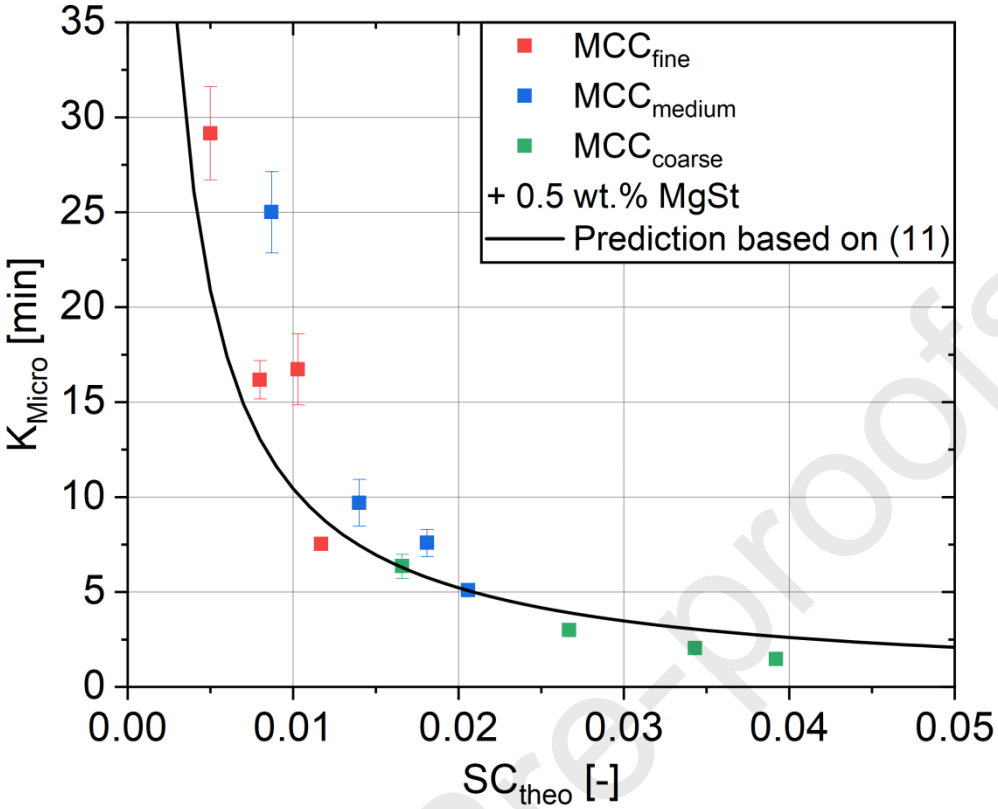

631

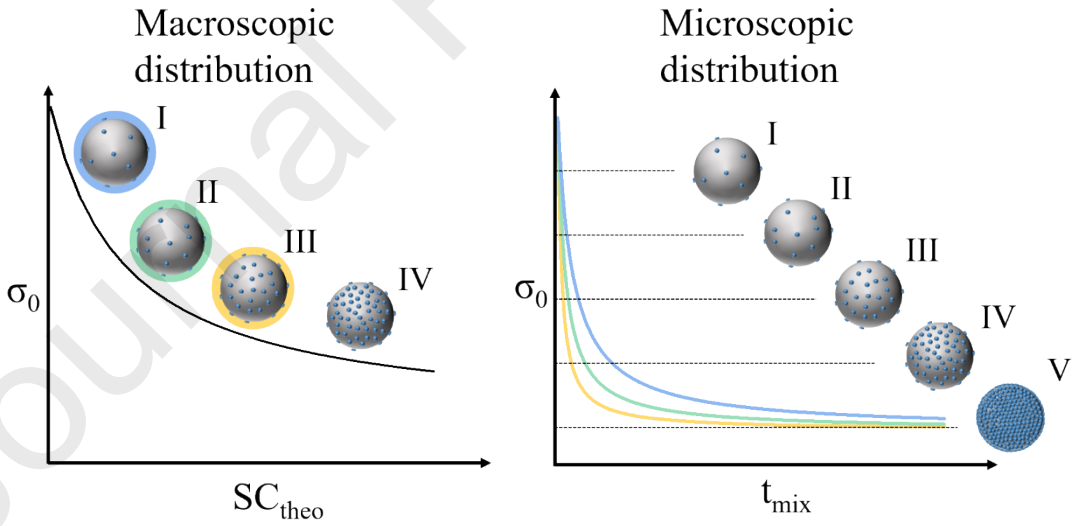

632

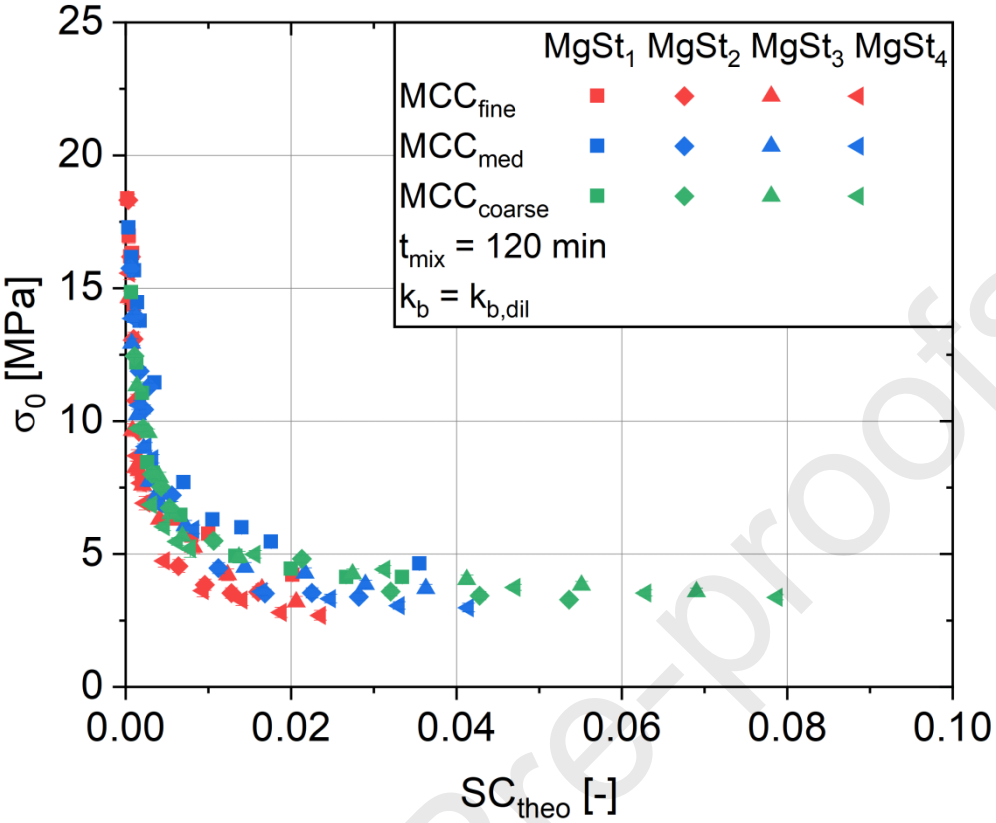

633